Support Information

Exploring antiviral and antiparasitic activity of gold N-heterocyclic carbenes with thiolate ligands

*Igor S. Oliveira[a], Marcus S. A. Garcia[b], Natasha M. Cassani[c], Ana L. C. Oliveira[c], Lara C. F. Freitas[c], Vitor K. S. Bertolini[b], Jennyfer C. da Silva[a], Gustavo C. Rodrigues[a], João Honorato[d], Fernanda R. Gadelha[b], Danilo C. Miguel[b], Ana C. G. Jardim[c], Camilla Abbehausen[a]**

[a] Institute of Chemistry, University of Campinas, Campinas, São Paulo, Brazil [b] Institute of Biology, University of Campinas, Campinas, São Paulo, Brazil [c] Laboratory of Antiviral Research (LAPAV), Institute of Biomedical Sciences, Federal University of Uberlândia [d] Institute of Chemistry, University of São Paulo

Table of contents

EXPERIMENTAL

Materials and equipment

All reagents of commercial grade were used without prior purification. The following reagents: potassium hydroxide, silver nitrate, 40% (w/w) glyoxal, 2,4,6-trimethylaniline, paraformaldehyde, chlorotrimethylsilane, tetrahydrothiophene, potassium tetrachloroaurate, 2-thiazoline-2-thione, 2-benzothiazolidine-2-thione, 2-pyrimidine-2-thione, 2-thiouracil, sodium methoxide, N-acetyl-cysteine, deuterated dimethyl sulfoxide (DMSO-d_6), calf thymus DNA (CT-DNA), dialysis membrane were acquired from Sigma-Aldrich. Potassium carbonate, methanol, dichloromethane, ethyl ether, and dimethyl sulfoxide were acquired from Synth. Bovine serum albumin (BSA) was acquired from Bio Basic Canada.

Elemental analyses were obtained on a Perkin Elmer 2400 CHNS/O Analyzer. Hydrogen (^{1}H) and proton-decoupled carbon (^{13}C{^{1}H}) nuclear magnetic resonance (NMR) spectra were acquired on Bruker Avance III 500/400/250 MHz instruments, samples were dissolved in deuterated dimethyl sulfoxide (DMSO-d6). Spectra generated from high-resolution mass spectrometry (HRMS) were acquired using the Thermo Q-Exactive Orbitrap instrument with electrospray ionization (ESI-MS) in positive acquisition mode. All samples were filtered and diluted in a methanol:water solution containing 0.1% v/v formic acid. Final solutions were directly injected into the instrument and analyzed in positive mode with a flow rate of 200 $\mu L \cdot min^{-1}$. The single crystal X-ray diffraction data were collected at 100 K using a Rigaku Synergy-S diffractometer with Mo Kα (λ = 0.71073) radiation and an HPC-type area detector (Hypix 6000HE). The initial unit cell parameters, collection planning, integration, and data reduction were calculated using the CrysAlisPro software. Molecular representations and crystallographic data tables were generated with OLEX2 and MERCURY programs[1,2].

The structures were solved using the SHELXT program through direct methods, and successive Fourier difference maps were used to locate non-hydrogen atoms[3]. All atoms, except hydrogen, were refined anisotropically. Refinements were conducted using the least squares method with the SHELXL program. Specific details regarding data collection and crystallographic parameters are provided in Table S1. Fluorescence spectra were obtained on a Cary Eclipse fluorescence spectrophotometer using a quartz cuvette with 4 polished sides and a 1.0 cm optical path, with average scanning speed. Circular dichroism spectra were obtained on a Jasco J-720 spectrophotometer with a 1.0 cm quartz cuvette optical path. Potentiometric titration was carried with an automatic titrator (Triton Plus 848) - Metrohm 801 Stirrer. The quantifications of gold were performed by ICP-OES model Perkin-Elmer Optima 8300.

Potentiometric titration of ligands SR

For the potentiometric studies, the ligand solutions were prepared in a concentration of 0.1 mol·L^{-1} for Stzn, Spym, and 2-tu; and 0.05 mol L^{-1} for Sbtz with a standardized basic solution of NaOH 0.1 mol·L^{-1}. The samples were titrated with a solution of HCl 0.1 mol·L^{-1} using a potentiometric titrator. The titration curves were analyzed with the CurTiPot 4.4.0 program to obtain the pKa values[4]. The experiments were performed in triplicate.

Octanol-water partition coefficient determination (logP) - Lipophilicity

The partition coefficients (log P) of the complexes in n-octanol:water were obtained, using the shake flask method according to OECD guidelines[5]. First, a saturated solution of water and n-octanol was prepared by stirring the two solvents together for 24 hours and separating the phases after that. Stock compound solutions (0.1 mmol·L^{-1} in 1% DMSO) were dissolved in 25 mL of saturated water. The samples were prepared by mixing 7.5 mL of stock solution with 7.5 mL of saturated n-octanol and mixed in an

orbital agitator at 1000 rpm for 2 h. Then, samples were centrifuged at 4200 rpm for 15 min. The aqueous phases (7.0 mL) were subjected to 1:1 (V/V) aqua regia treatment and heated until complete drying. The residue was calcined at 600 ºC for 20 min. The solids were dissolved with an aqueous solution of aqua regia 1% and the gold content in each replicate was quantified by ICP-OES. The concentration was calibrated with standard gold solution for ICP in HCl 1g L^{-1} (Supelco®).The partition coefficients (log P) were calculated using concentration data from both phases (Eq. 1), considering the concentration in octanol is the difference from stock solution and the concentration measured in water. The experiments were performed in duplicate.

$$loglog\ P = \frac{[Au]octanol}{[Au]water} \qquad \textbf{Eq. 1}$$

Synthesis of the complex AuIMesCl

The synthesis of the complex AuIMesCl was carried out according to the procedure described in the literature1. In a flask, 0.35 mmol of IMes·HCl and 0.35 mmol of Au(tht)Cl were added, along with 15.0 mL of dichloromethane (DCM). This solution was constantly stirred for 15 min. Then, 7.0 mmol of K_2CO_3 was added while keeping the system under constant stirring and protected from light for 1.5 h. The mixture was filtered through Celite, and the resulting solution was reduced to approximately 5.0 mL in volume. To this solution, 10.0 mL of cold ethyl ether was added dropwise, forming a white precipitate with a crystalline appearance, which was separated by filtration and washed with three portions of 5.0 mL of ethyl ether. The precipitate was dried under vacuum.

General procedure for the synthesis of gold complexes AuIMesSR

The general procedure for the substitution synthesis of chloride ligands on Au(I)(NHC) with thiolate ligands was adapted from the literature. In a flask, 0.06 mmol of the respective nitrogen base with a thiol group (HSR), 0.06 mmol of base (potassium

hydroxide or sodium methoxide), and 5.0 mL of methanol (MeOH) were added, resulting in a solution to which 0.06 mmol of the precursor complex AuIMesCl was added. The mixture was stirred constantly and protected from light at room temperature for 2 h. To remove potassium chloride from the product, the MeOH volume was removed using a rotary evaporator, and 5.0 mL of dichloromethane (DCM) was added to this flask, forming a suspension that was filtered through Celite. The resulting solution was concentrated under reduced pressure to a volume of approximately 2.0 mL, and then ethyl ether was added for precipitation, yielding a colorless solid with a crystalline appearance that was dried under vacuum.

Synthesis of the complex AuIMesStzn

The synthesis procedure of the complex AuIMesStzn was carried out according to the described general procedure, where 2-mercaptothiazoline (HStzn) and potassium hydroxide (KOH) were used as the base, yielding a colorless solid with a crystalline appearance at the end of the procedure. This complex can also be referred to as AuIMesStzn throughout the text. From elemental analysis, the empirical formula $AuC_{24}H_{28}N_3S_2{\cdot}{}^1/_2H_2O$ was proposed. Calculated (%): C 45.86, H 4.65, N 6.68. Experimental (%): C 45.75, H 4.55, N 6.60.

Synthesis of the complex AuIMesSbtz

The synthesis procedure of the complex AuIMesSbtz was carried out according to the described general procedure, where 2-mercaptobenzothiazole (HSbtz) and sodium methoxide (NaOMe) were used as the base, yielding a colorless solid with a crystalline appearance at the end of the procedure. This complex can also be referred to as AuIMesSbtz throughout the text. From elemental analysis, the empirical formula $AuC_{28}H_{28}N_3S_2{\cdot}H_2O$ was proposed. Calculated (%): C 49.05, H 4.41, N 6.13. Experimental (%): C 49.25, H 4.125, N 6.13.

Synthesis of the complex AuIMesSpym

The synthesis procedure of the complex AuIMesSpym was carried out according to the described general procedure, where 2-mercaptopyrimidine (HSpym) and sodium methoxide were used as the base, yielding a yellowish solid with a crystalline appearance at the end of the procedure. Monocrystals were obtained by slow evaporation of the reaction medium in methanol at a temperature of 5 °C. This complex can also be referred to as AuIMesSpym throughout the text. From elemental analysis, the empirical formula $AuC_{25}H_{27}N_4S\cdot{}^5/_3H_2O$ was proposed. Calculated (%): C 46.73; H 4.76; N 8.72. Experimental (%): C 46.70; H 4.29; N 8.41.

Synthesis of the complex AuIMes2tu

The synthesis procedure of the complex AuIMes2tu was carried out according to the described general procedure but using 2-thiouracil (2-tuH) and sodium methoxide as the base, yielding a colorless solid with a crystalline appearance at the end of the procedure. Monocrystals were obtained by slow evaporation of the reaction medium in methanol at a temperature of 5 °C. This complex can also be referred to as AuIMes2tu throughout the text. From elemental analysis, the empirical formula $AuC_{25}H_{27}N_4OS\cdot{}^3/_2H_2O$ was proposed. Calculated (%): C 45.80, H 4.61, N 8.55. Experimental (%): C 45.94, H 4.24, N 8.36.

Computational Methods

To gain deeper insight into the thermodynamics governing the equilibria of gold compounds with N-acetylcysteine (NAC), Density Functional Theory (DFT) calculations were performed using the ORCA package (version 5.0.3)[6,7]. The objective was to determine the Gibbs Free Energy variation (ΔG) for the reactions involving AuIMesCl, AuIMes2tu, AuIMesSbtz, AuIMesSpym, and AuIMesStzn interacting with NAC.

All reactants and products had their structures optimized, including the gold complexes (AuIMesCl, AuIMes2tu, AuIMesSbtz, AuIMesSpym, and AuIMesStzn), NAC in the protonated form (NACH), and the protonated leaving ligands (HCl, 2-tuH, HSbtz, HSpym, and HStzn). For 2-tuH, HSbtz, HSpym and HStzn, both thioamide and thioiminol tautomers were considered, for further stability comparison. The Gibbs Free Energy variation was then calculated based on the difference in free energy of products ([Au(IMes)(NAC)], and HX, the ligand in the protonated form) and reactants (NACH [Au(IMes)(X)], where X = Cl, 2tu, Sbtz, Spym and Stzn).

Frequency calculations were performed for the optimized structures, to certify convergence of optimized structures to local minima (via the absence of imaginary frequencies) and to calculate thermodynamic data, at 298.15 K. All calculations were conducted employing PBE0 functional[8], SARC-ZORA-TZVP basis set for Au(I) cations[9] for the inclusion of relativistic corrections, ZORA-def2-TZVP basis functions for other atoms, SARC/J auxiliary basis functions, RIJCOSX approximation[10], CPCM for implicit DMSO solvation[11], and a convergence criterion of 1.0 10^{-8} a.u.

Time dependent ^{1}H NMR analysis of the reaction between AuIMesSR and N-acetyl-L-cysteine (NAC)

A solution of each AuIMesSR were prepared at a concentration of 27.0 mmol·L^{-1}, of with DMSO-d_6. A stock solution of NAC in DMSO-d_6 was prepared at a concentration of 210.0 mmol·L^{-1}. In each NMR tube it was added 650 μL of AuIMesSR solution and 50 μL of the NAC stock solution, the mixture was homogenized using a vortex mixer resulting in a final concentration of 25.0 mmol·L^{-1} for both compounds and a total volume of 700 μL. This procedure aimed to establish an equimolar ratio of each reagent 1:1(gold complex:NAC). The time interval between the addition of the NAC stock solution and the start of the ^{1}H NMR measurement was approximately 5 minutes. Spectra were

recorded at 25 °C at specific intervals: 0 h, 3 h, 6 h, 9 h, 12 h, 15 h, 18 h, and 24 h. Each measurement was obtained through four scans with a relaxation time of 60 seconds, using a Bruker Avance 400 MHz instrument.

Calculation of Percentage of Volume Buried and Steric Maps

The structures used in these calculations were derived from the crystallographic data of the AuIMesSR series discussed in this work, specifically CCDC entries 2363392, 2363393, 2363394, and 2363395. For each structure, the metal center was chosen as the origin point, with the xz-plane aligned with the plane of the imidazole ring in the IMes ligand (Figure S33). The parameters applied were consistent with those reported in the literature[12]. The radius R of the sphere surrounding the metal core was set to 3.5 Å, and a mesh with a resolution of 0.1 Å was used to scan the sphere for buried voxels, utilizing Bondi radii scaled by 1.17. Van der Waals radii were employed, and hydrogen atoms were excluded from the steric map calculations. The percentage of buried volume and the steric maps were generated using the SambVca 2.1 Web application[13].

Interaction Studies with Bovine Serum Albumin by Fluorescence Quenching

Samples with a volume of 2.50 mL of a BSA solution at a concentration of 20.0 $\mu mol \cdot L^{-1}$, prepared in a 50 $mmol \cdot L^{-1}$ phosphate buffer solution at pH 7.4, were titrated with successive additions of 2.0 µL of a complex solution dissolved in DMSO at a concentration of 1.50 $mmol \cdot L^{-1}$. The addition of this solution did not significantly alter the final concentration of BSA. The intrinsic fluorescence emission of BSA was monitored in the range of 300 to 450 nm with excitation at 280 nm at 25 °C, using 5 nm excitation and emission slits.

Interaction Study with CT-DNA by Circular Dichroism

Samples of calf thymus DNA (CT-DNA) at 100 $\mu mol \cdot L^{-1}$, prepared in a 10 $mmol \cdot L^{-1}$ phosphate buffer at pH 7.4, were incubated at 37 °C for 24 h with solutions of

gold(I) complexes in DMSO at different [compound]/[DNA] ratios (ranging from 0 to 0.50) for a total volume of 2.0 mL and a final concentration of 1% (v/v) DMSO. A control sample of CT-DNA at 100 μmol·L^{-1} in 10 mmol·L^{-1} phosphate buffer at pH 7.4 and 1% DMSO was used. The spectra were acquired at a scanning speed of 50 nm·min^{-1}, with 8 accumulations at 37 °C.

Parasites

Leishmania (*L.*) *amazonensis* (IFLA/BR/67/PH8) promastigotes were cultivated at 25 °C in 25 cm^2 tissue culture flasks containing M199 medium (Gibco-BRL, Invitrogen®) supplemented as described[14]. Cultures were split every 5 days, after promastigotes reach late logarithmic growth phase.

Trypanosoma (T.) cruzi (Y strain) epimastigotes were cultivated at 28 °C in liver infusion tryptose (LIT) medium, supplemented with 20 mg·L^{-1} hemin, 10% fetal bovine serum (Cutilab®), 50 U·mL^{-1} penicillin and 50 μg·mL^{-1} streptomycin (Invitrogen®).

Extraction of primary host cell

Bone marrow-derived macrophages (BMDM) were obtained after differentiation of precursor cells extracted from femurs and tibias of female Balb/C mice. The medullary cavities of the bones were washed with a 5 mL syringe and a 21G needle with Roswell Park Memorial Institute (RPMI 1640) medium (Gibco-Invitrogen) supplemented with 20% FBS and 30% L929 fibroblast culture supernatant in 75 mm Petri dishes. Recovered cells were kept at 37 ºC with 5% CO_2 atmosphere. After 7 days, differentiated BMDM were collected with fresh RPMI medium after scraping the plate with a sterile cell scraper (Biofil®). The Ethics Committee on Animal Use of the University of Campinas (CEUA-UNICAMP) (protocol 6022-1/2022) approved all procedures using mice.

Parasites and BMDM assays

Cell viability was evaluated by the MTT ((3-(4,5-dimethylthiazol-2-yl)-2,5-diphenyltetrazolium bromide) assay[15] using log phase *Leishmania* promastigote or *T. cruzi* epimastigotes cultures (5×10^6 cells/well) or BMDM (5×10^4 cells/well) in 96-well culture plates incubated with decreasing concentrations of the Au complexes (100; 50; 25; 12.5; 6.25; 3.13; 1.56; 0 μM) for 24 h. The ligands HStzn, HSbtz, HSpym, and 2-tuH were also tested in parallel to exclude leishmanicidal activity in each case, along with a group containing up to 1% (v/v) DMSO as a diluent control. All complexes and ligands were freshly solubilized in pure sterile DMSO (Sigma Aldrich) at 10 mM stocks for each experiment. Briefly, 30 μL of MTT (5 $mg \cdot mL^{-1}$) was added to each well and the plates were incubated for 3 h at 25 ºC (for promastigotes and epimastigotes) and 37 ºC (for macrophages). Next, the reaction was stopped by addition of 30 μL of SDS 20%. Absorbance reading was performed using a plate spectrophotometer (reference and test wavelength of 600 and 650 nm, respectively). Optical density values were converted to percentages compared to untreated control groups incubated with medium only (100% viability) to determine the 50% effective concentrations (EC_{50} for parasites and CC_{50} for macrophages) from sigmoidal regression of dose-response curves (GraphPad Prism8 software, USA).

In vitro* infections with *L. amazonensis

To assess the viability of intracellular amastigotes, 4×10^5 BMDM were cultured in each well containing 13 mm glass coverslip in 24-well plates. Next, cells were incubated with stationary phase promastigotes of *L. amazonensis* (5 parasites: 1 macrophage) for an overnight period at 34 ºC and 5% CO_2 and then exposed or not to increasing concentrations of the gold compounds for 24 h. Coverslips were fixed with

pure methanol and stained with an Instant Prov kit (NewProv, Brazil). The number of infected cells and amastigotes per 300 BMDM were quantified microscopically by direct counting as described[16]. Infection rates (%) were determined as the proportion of BMDM containing at least one intracellular parasite in a total of 100 infected and non-infected BMDM. Inhibition data of intracellular amastigote multiplication were tallied in biological triplicates.

Vero E6 cell culture

Vero E6 cells (Kidney tissue derived from an African green monkey, ATCC E6) were cultured in modified Dulbecco's Modified Eagle Medium (DMEM; Sigma-Aldrich) supplemented with 100 $U \cdot mL^{-1}$ penicillin (Gibco Life Technologies), 100 $\mu g \cdot mL^{-1}$ streptomycin (Gibco Life Technologies), 1% (v/v) non-essential amino acids (Gibco Life Technologies), and 10% (v/v) fetal bovine serum (FBS; Hyclone) at 37 °C in a humidified 5% CO_2 incubator.

Vero E6 cell viability assay - MTT assay

Cell viability was measured by the MTT method (Sigma-Aldrich). Vero E6 cells were seeded in 96-well plates at a density of $5 \cdot 10^3$ cells per well for ZIKV assays, $2 \cdot 10^4$ cells per well in 48-well plates for MAYV-*nanoluc* assays, and $1 \cdot 10^4$ cells per well in 96-well plates for VSV-eGFP-SARS-CoV-2-S. Cells were incubated overnight at 37 °C in a 5% CO_2 humidified incubator. To the cell culture medium, solutions of the gold complexes at concentrations of 50, 10, and 2 μM were added, and these solutions were incubated with these cells at 37 °C for different periods, 24, 48, and 72 h, respectively, corresponding to the infection assay time for each virus. Then, the medium was removed, and a 1 $mg \cdot mL^{-1}$ MTT solution was added to each well and incubated for 30 min at 37 °C in a 5% CO_2 humidified incubator. Then, the medium was replaced with 100 μL of DMSO to solubilize the formazan crystals. Subsequently, absorbance was measured by optical

density (OD) of each well at 560 nm using the Glomax microplate reader (PROMEGA). Cell viability was calculated according to the equation (T/C) × 100%, where T and C represent the mean optical density of the treated group and the vehicle control group, respectively. Data were analyzed for normal distribution to demonstrate the applicability of parametric or non-parametric tests. Then, two-way ANOVA test was employed to compare the treatment of each compound with the DMSO control, with a $p < 0.05$.

Antiviral activity assays - ZIKV

A wild-type ZIKV sample isolated from a clinical sample from a patient in Brazil ($ZIKV_{PE243}$) was amplified using Vero E6 cells in a 75 cm² flask for 3 days. Then, the viral supernatant was collected and stored at -80 °C. To determine viral titers, $5 \cdot 10^3$ Vero E6 cells were seeded in each well of 96-well plates for 24 h before infection. The cells were infected with a tenfold serial dilution of $ZIKV_{PE243}$ and incubated for 72 h in a humidified 5% CO_2 incubator at 37 °C. Then, the cells were fixed with 4% (v/v) formaldehyde, washed with PBS [1x], and added with blocking buffer (BB) containing 0.1% (v/v) Triton X-100, 0.2% (w/v) BSA, and PBS for 30 min, for immunofluorescence assay as previously described[17].

To evaluate the antiviral activity of each compound, Vero E6 cells were seeded at a density of $5 \cdot 10^3$ cells per well in 96-well plates for 24 h, and then infected with $ZIKV_{PE243}$ at a multiplicity of infection (MOI) of 0.01 in the presence of each compound at the established non-cytotoxic concentration for 72 h. The cells were fixed with 4% (v/v) formaldehyde, washed with PBS [x1], and added with BB for immunofluorescence assay. Focus-forming units (FFU) were measured at EVOs cell fluorescence microscopy (Thermo Fisher Scientific) and calculated according to the equation (T/C) × 100%, where T and C represent the mean optical density of the treated group and the vehicle control group, respectively. Data were analyzed for normal distribution to demonstrate the

applicability of parametric or non-parametric tests. Then, two-way ANOVA test was employed to compare the treatment of each compound with the DMSO control, with a $p < 0.05$.

Antiviral activity assays – MAYV

MAYV-*nanoluc* was produced and rescued as previously described (In Press). To determine viral titers, 8×10^4 Vero E6 cells/well were seeded in 24 wells plate, and 24 h later, the cells were infected with ten-fold serial dilutions of each MAYV infectious clone. Cells were incubated with viruses for 1 h at 37 °C and 5% CO_2, followed by the inoculum removal, washes with PBS to remove the unbound virus, and addition of fresh medium supplemented with 1% dilution of stock of penicillin and streptomycin, 2% FBS, and 1% carboxymethyl cellulose (CMC). Infected cells were incubated for 2 days in a humidified 5% CO_2 incubator at 37 °C, followed by fixation with 4% formaldehyde and staining with 0.5% violet crystal. The viral foci were visualized to determine plaque morphology. Images were analyzed at EVOs M5000 Cell Imaging Systems (Thermo Fisher Scientific) (In Press).

To evaluate the antiviral activity of the compounds, Vero E6 cells were seeded at a density of $2 \cdot 10^4$ cells per well in 48-well plates. After 24 h, cells were infected with MAYV-*nanoluc* in the presence of each compound at its highest non-cytotoxic concentration for 48 h. Then, samples were harvested with Renilla-luciferase lysis buffer (Promega), and the levels of viral replication were quantified by measuring the *nanoluciferase* activity using the *Renilla*-luciferase assay (Promega) with a Glomax microplate reader (Promega). The antiviral activity was calculated according to the equation $(T/C) \times 100\%$, where T and C represent the mean of the treated group and the vehicle control group, respectively. Data were analyzed for normal distribution to demonstrate the applicability of parametric or non-parametric tests. Then, two-way

ANOVA test was employed to compare the treatment of each compound with the DMSO control, with a $p < 0.05$.

Antiviral activity assays - VSV-eGFP-SARS-CoV-2-S

Pseudotyped vesicular stomatitis virus (VSV) expressing eGFP as a marker for infection, in which the glycoprotein (G) gene was replaced by the spike protein (S) of SARS-CoV-2 (VSV-eGFP-SARS-CoV-2-S). The virus was expanded using Vero E6 cells in 175 cm^2 culture bottles, and after 48 h, the supernatant was collected to obtain aliquots for virus storage. To determine viral titers, $1 \cdot 10^4$ Vero E6 cells were cultured in 96-well plates 24 h before infection. After cell adhesion, cells were infected with VSV-eGFP-SARS-CoV-2-S in tenfold serial dilutions. The infected cells were incubated for 24 hours in a humidified incubator with 5% CO_2 at 37 °C. Viral foci were counted using fluorescence microscopy of EVOs cell imaging systems (Thermo Fisher Scientific), detecting eGFP expression, to determine the viral titer expressed in $ffu \cdot mL^{-1}$.

For antiviral assays, Vero E6 cells were seeded at a density of $1 \cdot 10^4$ cells per well in 96-well plates 24 h before infection. Samples of VSV-eGFP-SARS-CoV-2-S at a multiplicity of infection (MOI) of 0.001 and solutions of gold complexes at predetermined non-toxic concentrations in cell viability assays were pre-incubated for 1 h at room temperature. Then, cells were infected with VSV-eGFP-SARS-CoV-2-S and the compounds at 37 °C for 2 h. The supernatant was removed, and the cell monolayers were gently washed with 100 μL of ice-cold PBS [x1], and the wells were topped up with 2% DMEM culture medium. After 24 hours post-infection (h.p.i.), the assays were analyzed using EVOs cell fluorescence microscopy (Thermo Fisher Scientific), and the infection foci were counted. The antiviral activity was calculated according to the equation (T/C) × 100%, where T and C represent the mean of the treated group and the

vehicle control group, respectively. Two-way ANOVA test was performed to compare the effect of each compound on viral infection, $p < 0.05$ was considered significant.

Ligands Characterization

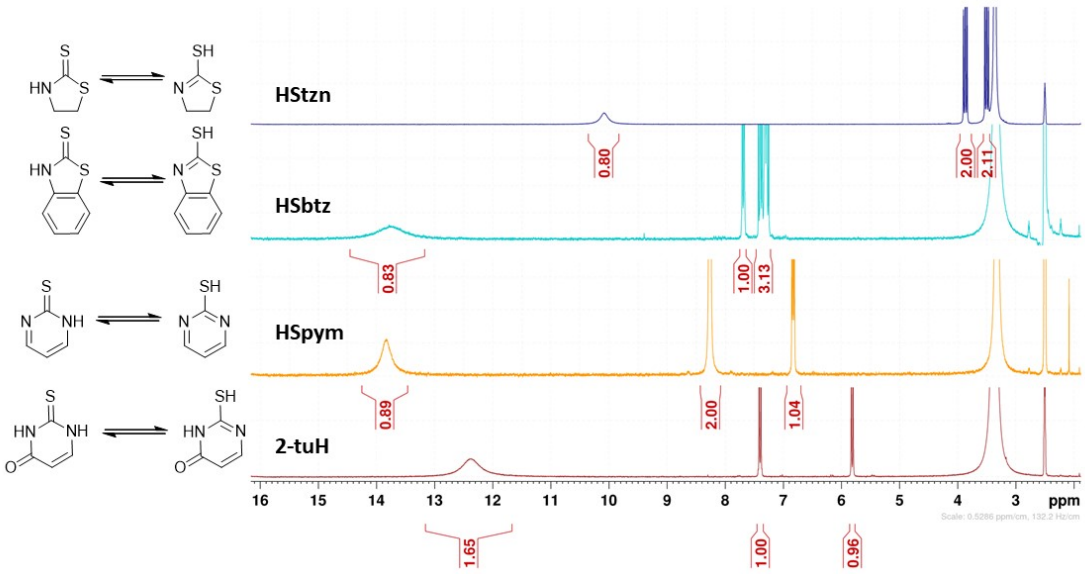

Figure S1. Tautomeric equilibrium of HStzn, HSbtz, HSpym, and 2-tuH in DMSO-d_6. ^{1}H NMR was acquired in DMSO-d_6 at 250 MHz and 25 °C, referenced to TMS and adjusted by the residual solvent signal. Spectra shown from 2.0 to 16.0 ppm. The NH signal is seen in the region of 12.0 to 14.5 ppm and integrated. Integrals reveal the amount of thione isomer present in solution.

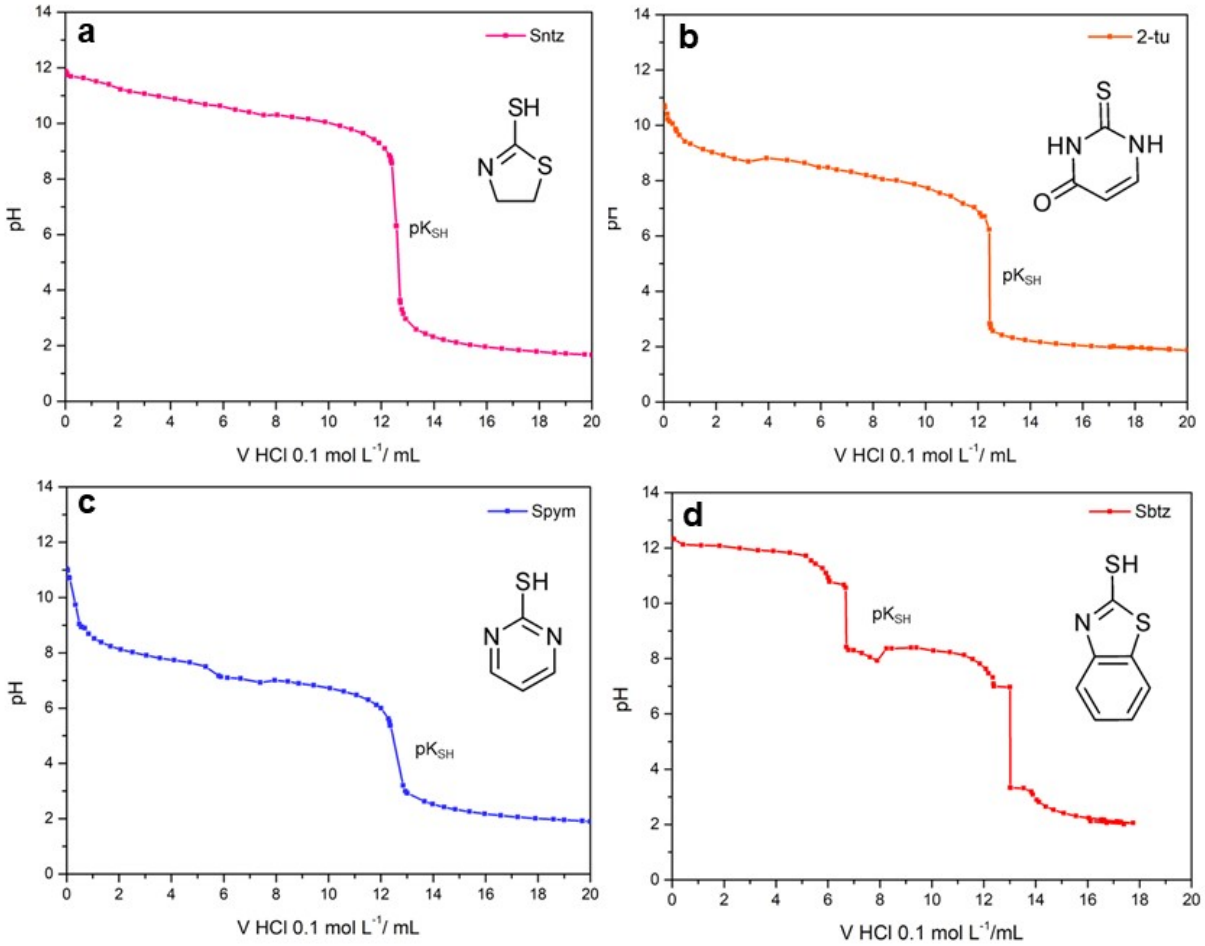

Figure S2. Potentiometric titration curves in HCl 0.1 mol L^{-1}. a) Titration of Stzn 0.1 mol L^{-1}. b) Titration of 2-tu 0.1 mol L^{-1}. c) Titration of Spym 0.1 mol L^{-1}. d) Titration of Sbtz 0.05 mol L^{-1}.

Complexes Characterization - NMR

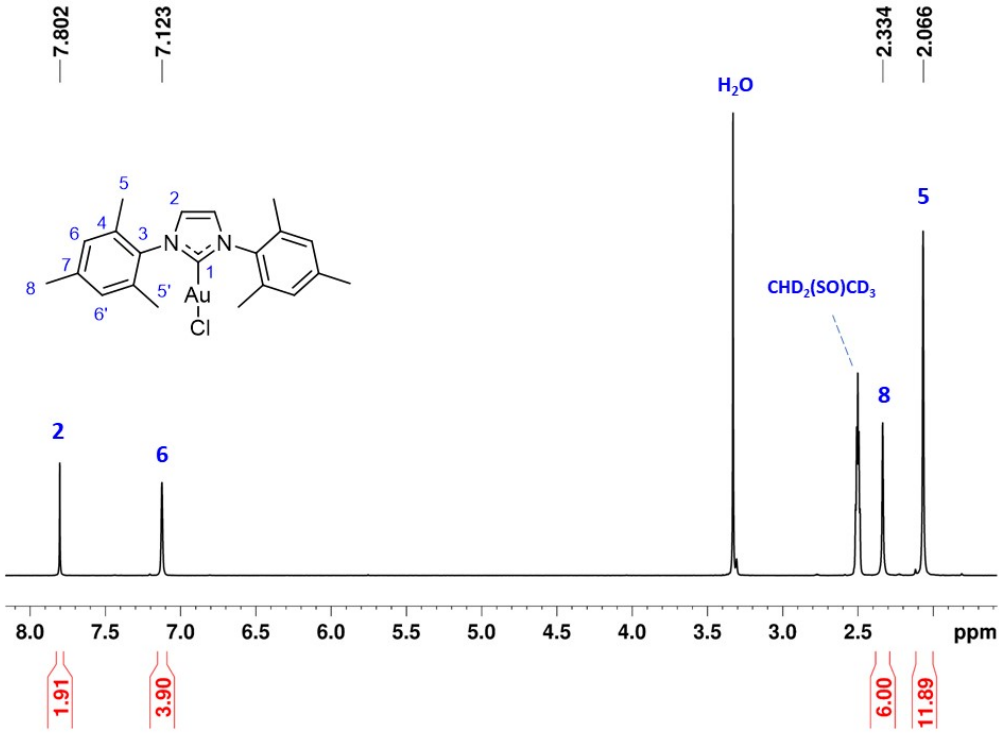

Figure S3. ^{1}H NMR spectrum of the AuIMesCl complex in DMSO-d_6 at 250 MHz.

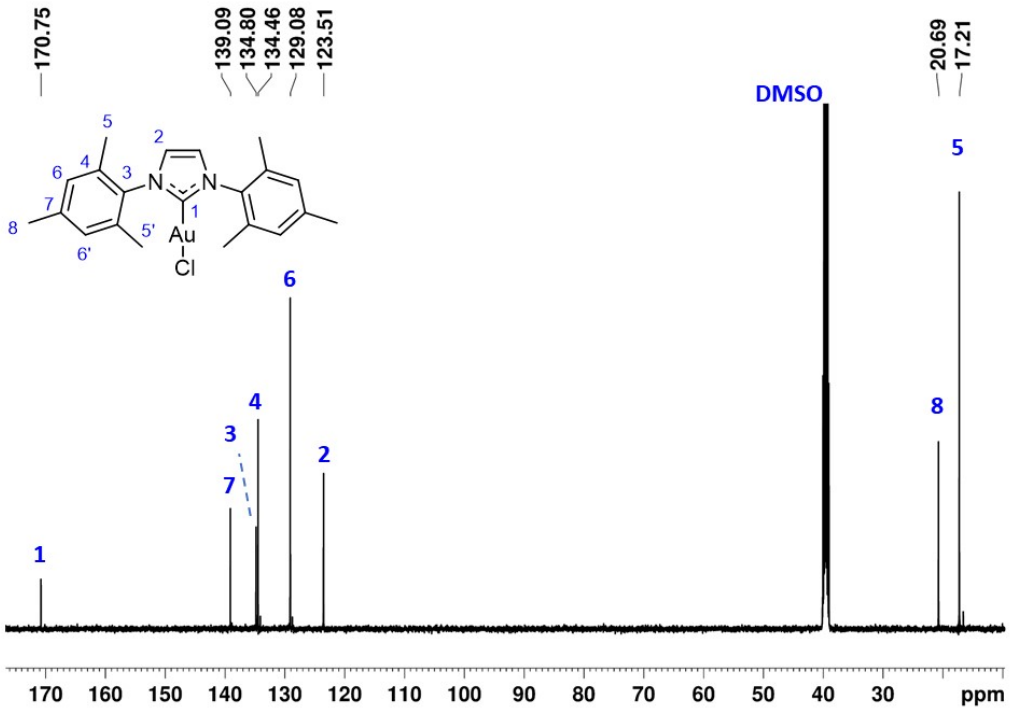

Figure S4. $^{13}C\{H^{1}\}$ NMR spectrum of the AuIMesCl complex in DMSO-d_6 at 500 MHz (^{1}H 499.9 MHz, ^{13}C 125.7 MHz).

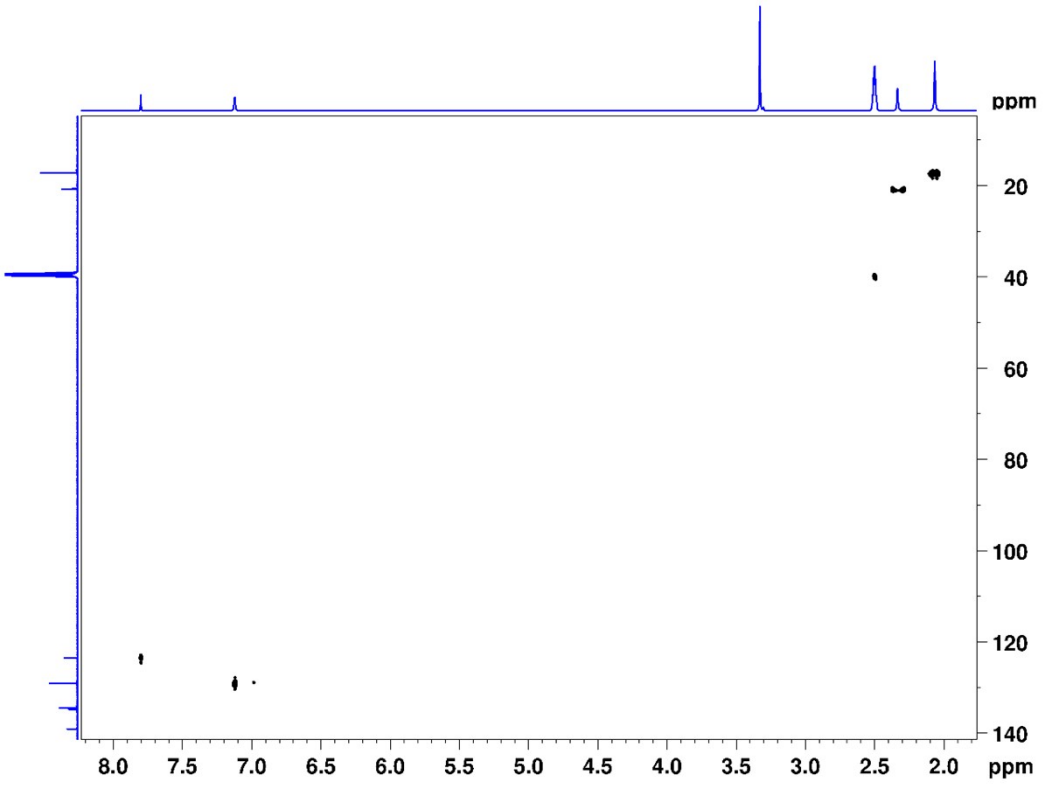

Figure S5. HSQC {^{1}H, ^{13}C} NMR Spectrum of the AuIMesCl complex at 500 MHz (^{1}H 499.9 MHz, ^{13}C 125.7 MHz) in DMSO-d_6.

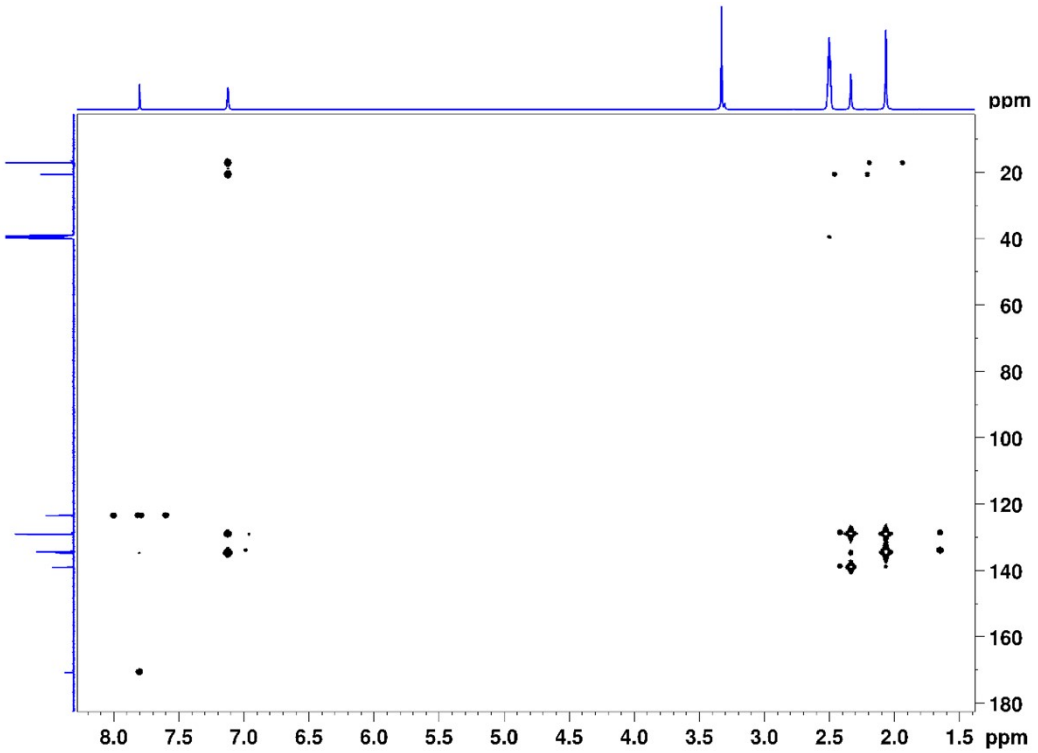

Figure S6. HMBC {^{1}H, ^{13}C} NMR Spectrum of the AuIMesCl complex at 500 MHz (^{1}H 499.9 MHz, ^{13}C 125.7 MHz) in DMSO-d_6.

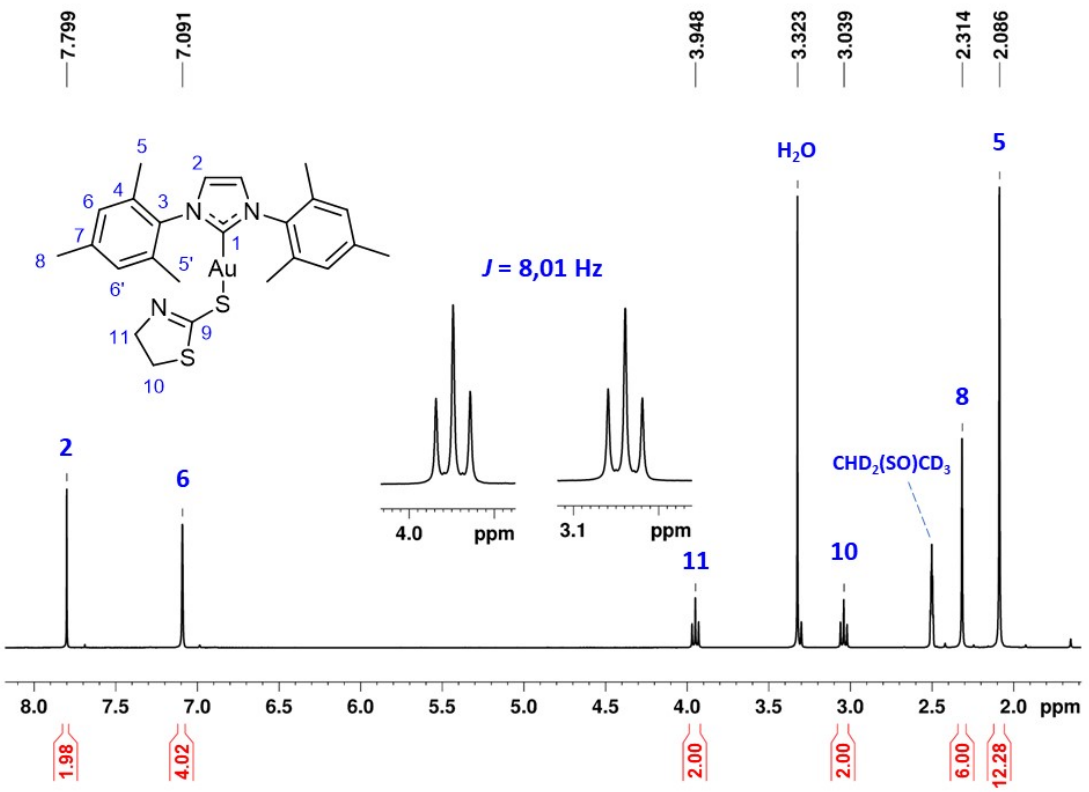

Figure S7. ^{1}H NMR spectrum of the AuIMesStzn complex in DMSO-d_6 at 400 MHz.

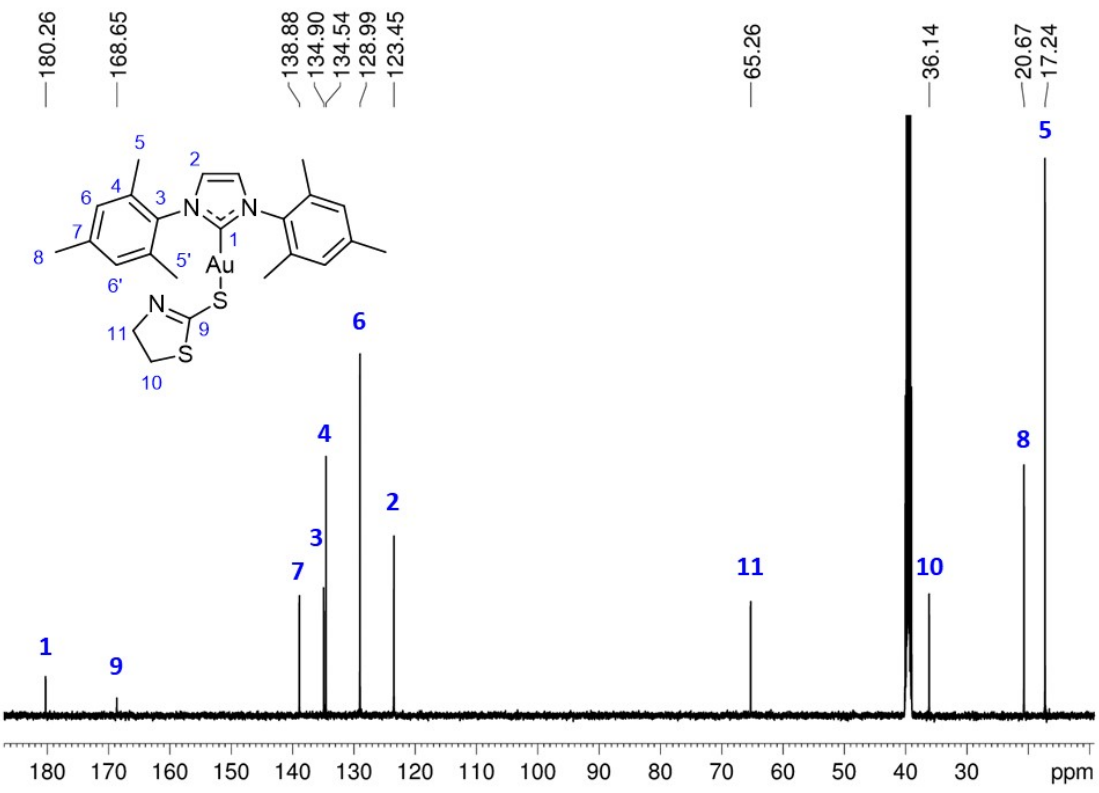

Figure S8. $^{13}C\{H^1\}$ NMR spectrum of the AuIMesStzn complex in DMSO-d_6 at (^1H 499.9 MHz, ^{13}C 125.7 MHz) 500 MHz.

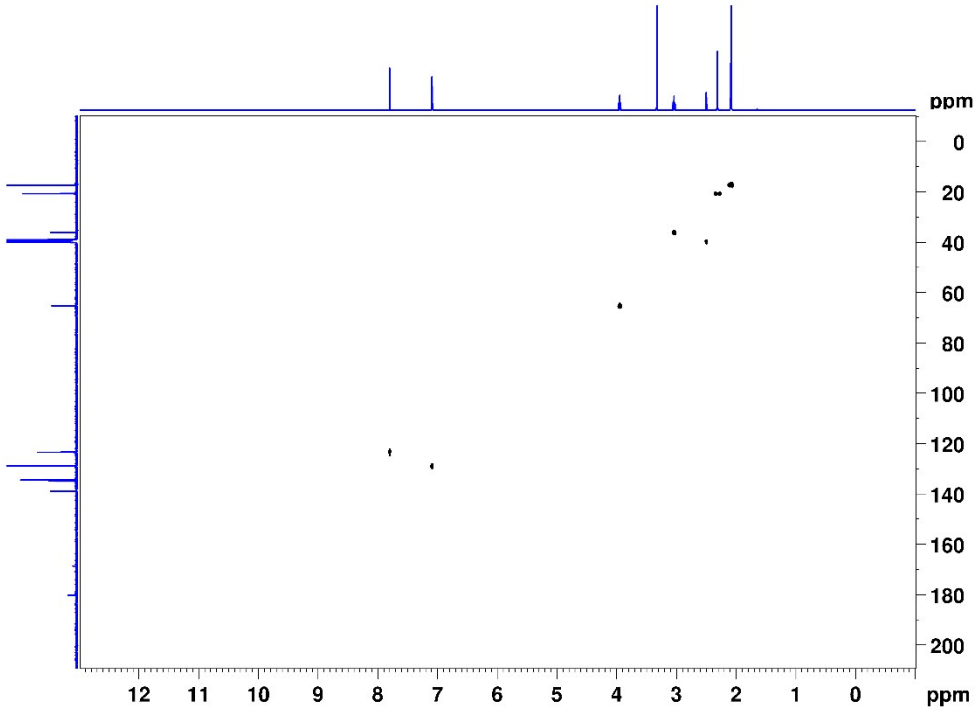

Figure S9. HSQC {^1H, ^{13}C} NMR Spectrum of the AuIMesStzn complex at 500 MHz (^1H 499.9 MHz, ^{13}C 125.7 MHz) in DMSO-d_6.

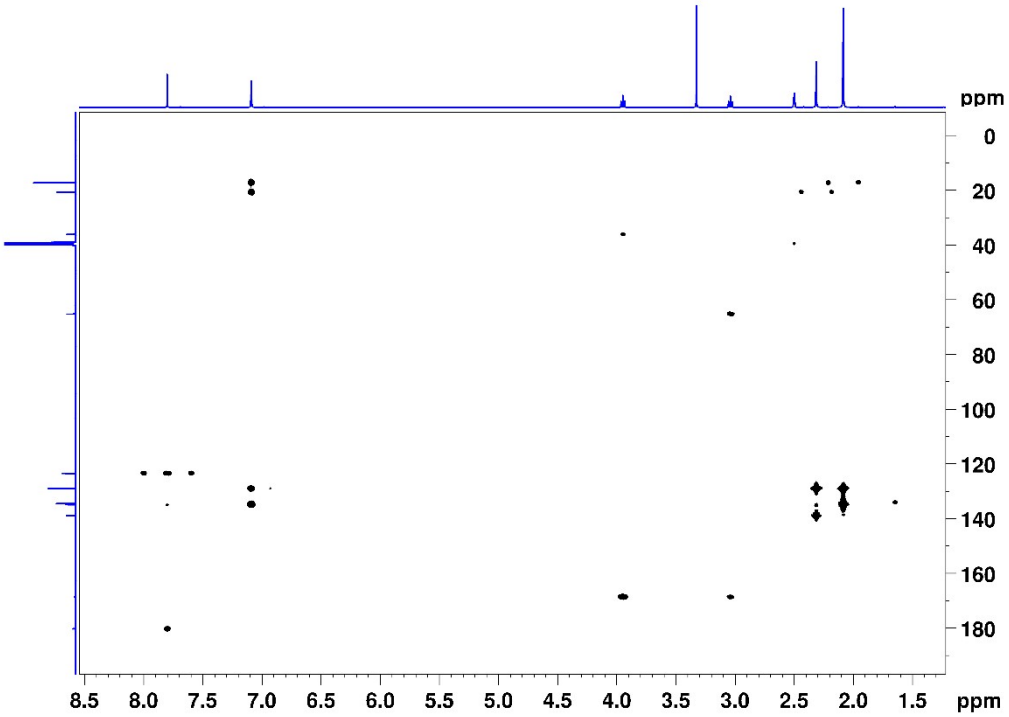

Figure S10. HMBC {^{1}H, ^{13}C} NMR Spectrum of the AuIMesStzn complex at 500 MHz (^{1}H 499.9 MHz, ^{13}C 125.7 MHz) in DMSO-d_6.

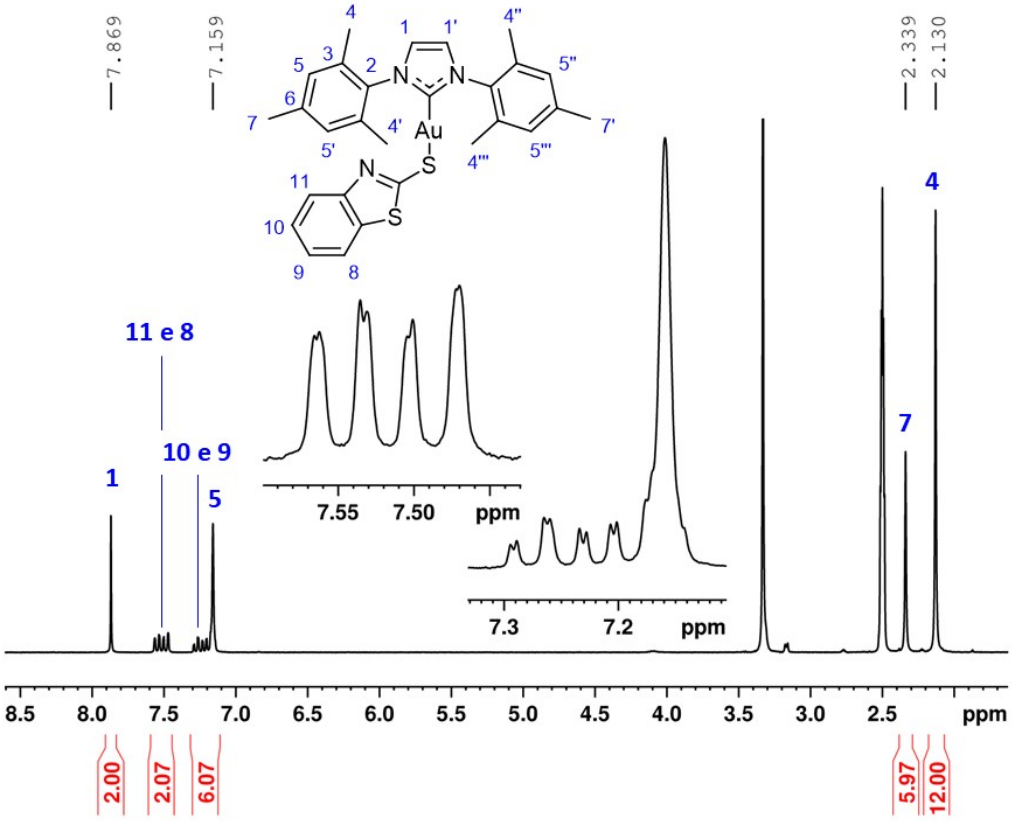

Figure S11. ^{1}H NMR spectrum of the AuIMesSbtz complex in DMSO-d_6 at 250 MHz.

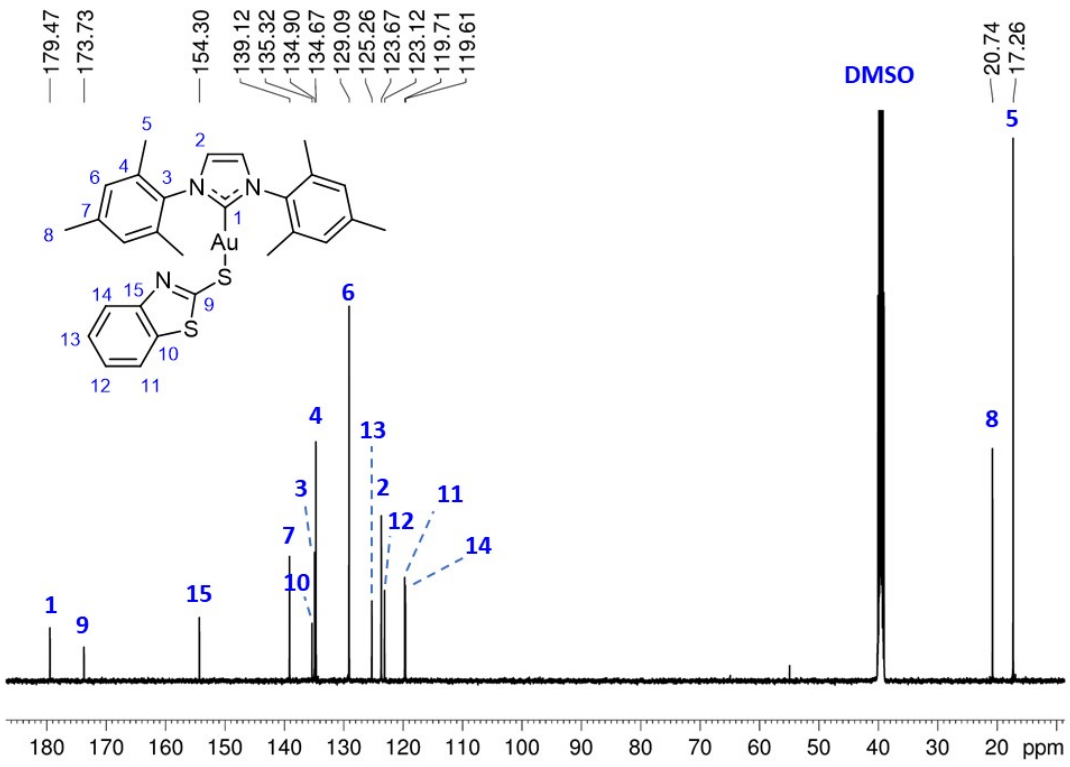

Figure S12. $^{13}C\{H^1\}$ NMR spectrum of the AuIMesSbtz complex in DMSO-d_6 at 500 MHz (^{13}C 125.7 MHz).

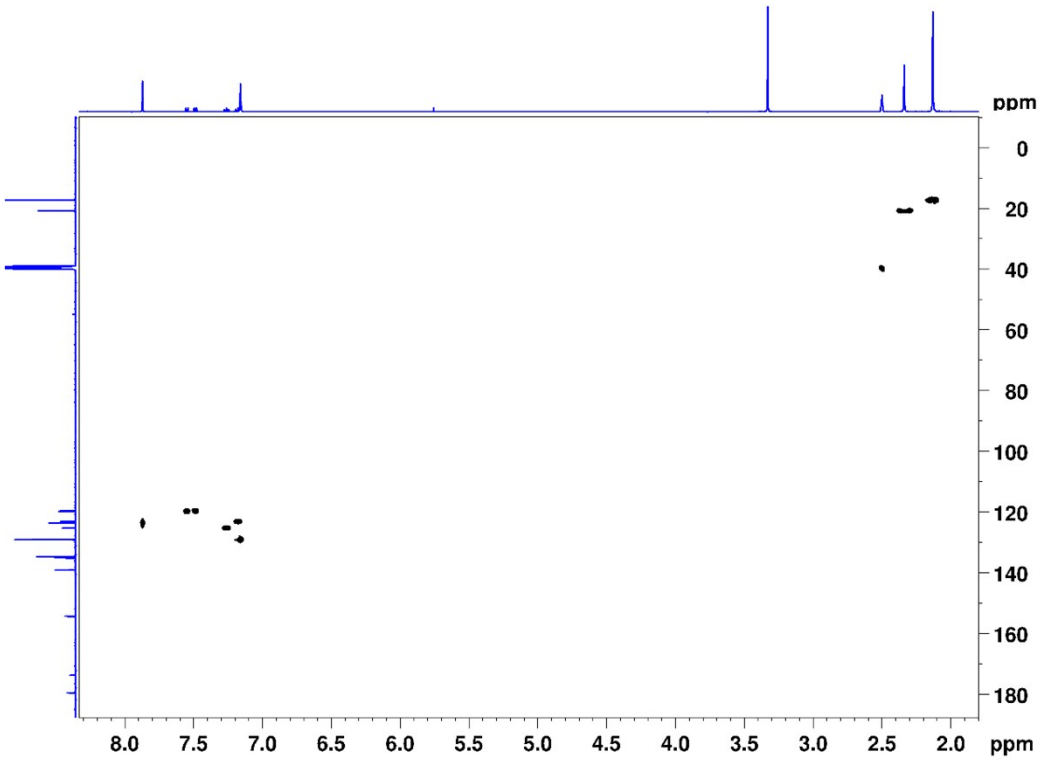

Figure S13. HSQC {^1H, ^{13}C} NMR Spectrum of the AuIMesSbtz complex at 500 MHz (^1H 499.9 MHz, ^{13}C 125.7 MHz) in DMSO-d_6.

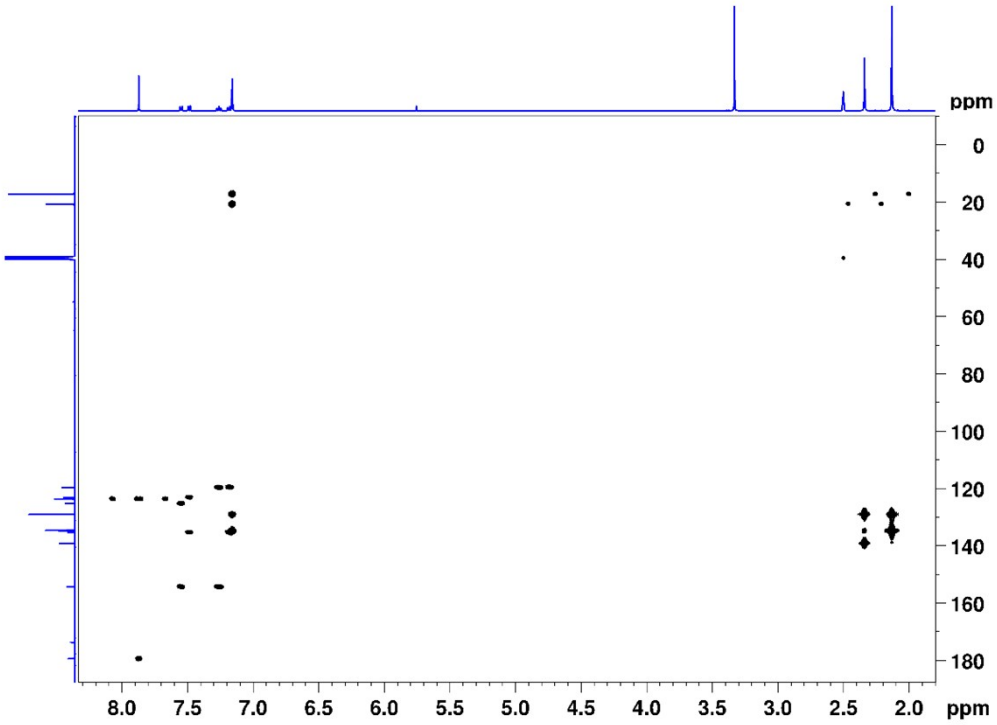

Figure S14. HMBC {^{1}H, ^{13}C} NMR Spectrum of the AuIMesSbtz complex at 500 MHz (^{1}H 499.9 MHz, ^{13}C 125.7 MHz) in DMSO-d_6.

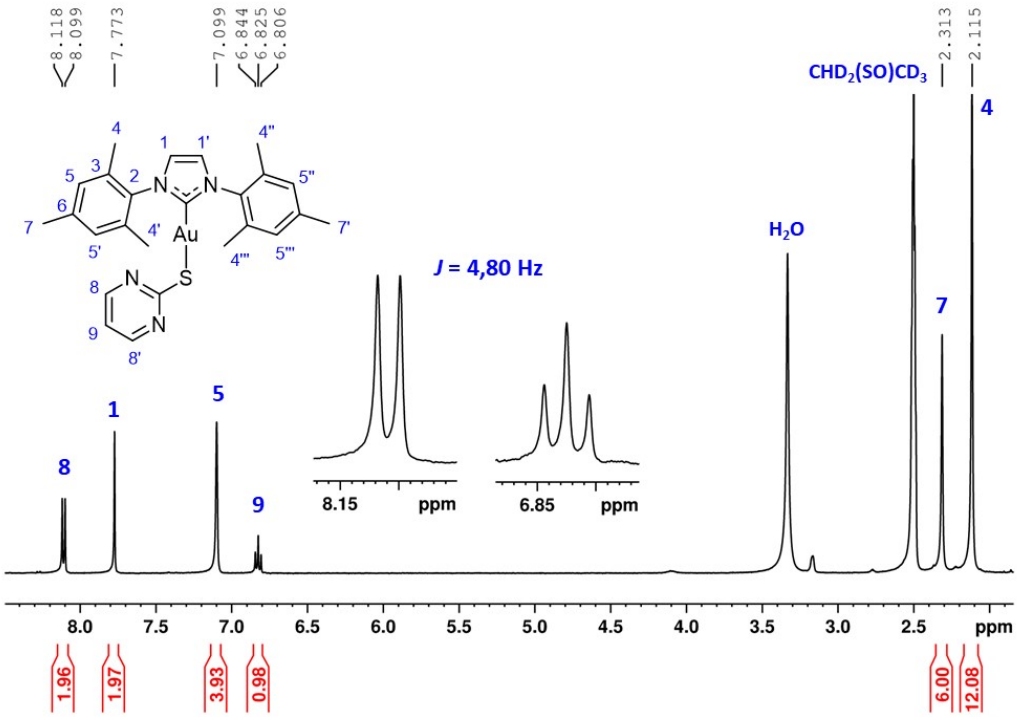

Figure S15. ^{1}H NMR spectrum of the AuIMesSpym complex in DMSO-d_6 at 250 MHz.

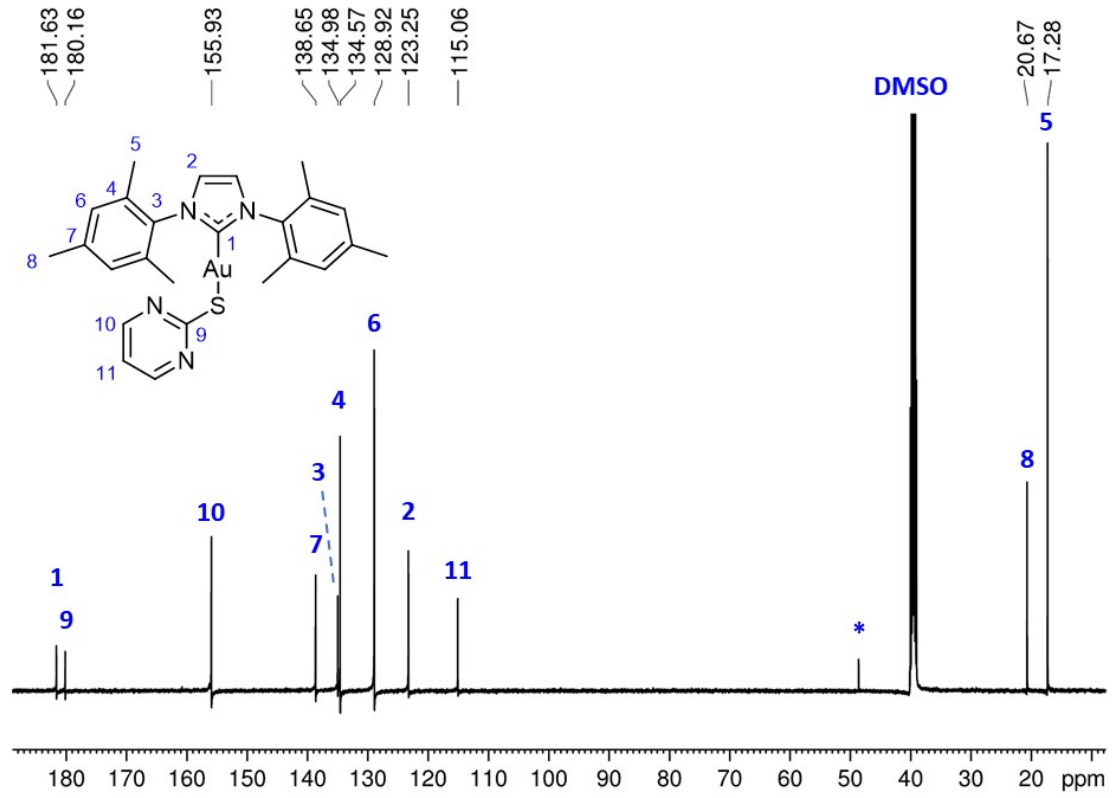

Figure S16. $^{13}C\{H^{1}\}$ NMR spectrum of the AuIMesSpym complex in DMSO-d_6 at 500 MHz (^{13}C 125.7 MHz).

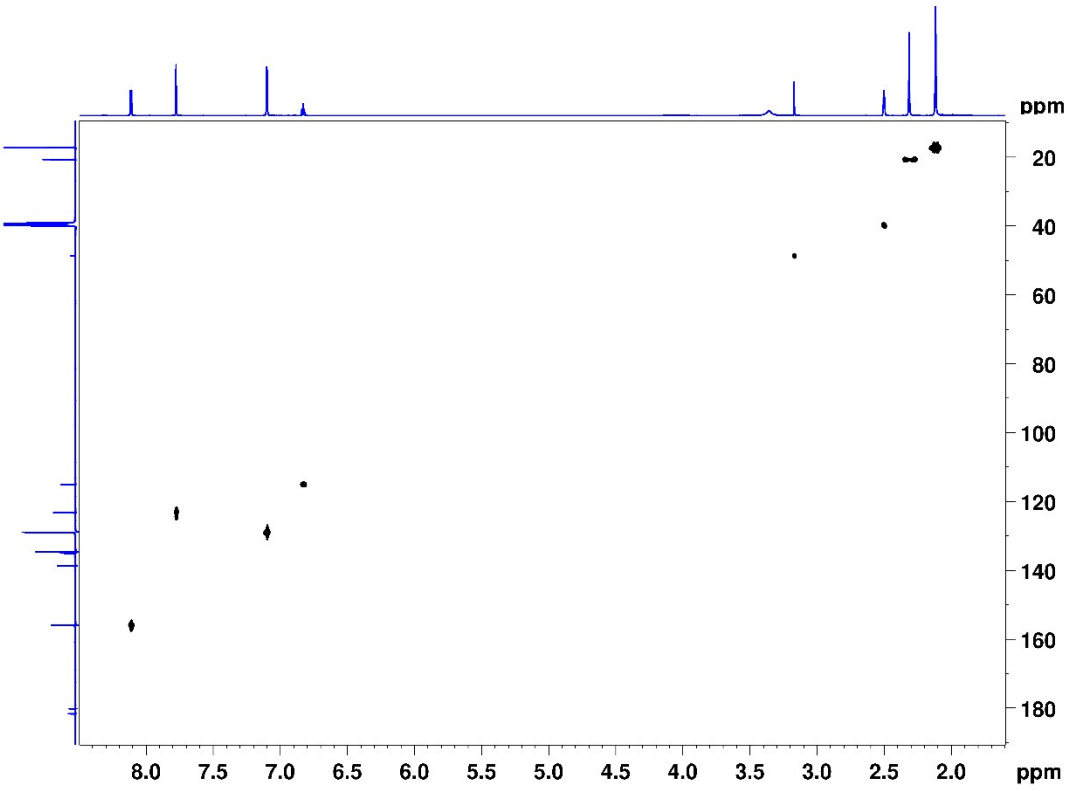

Figure S17. HSQC {^{1}H, ^{13}C} NMR Spectrum of the AuIMesSpym complex at 500 MHz (^{1}H 499.9 MHz, ^{13}C 125.7 MHz) in DMSO-d_6.

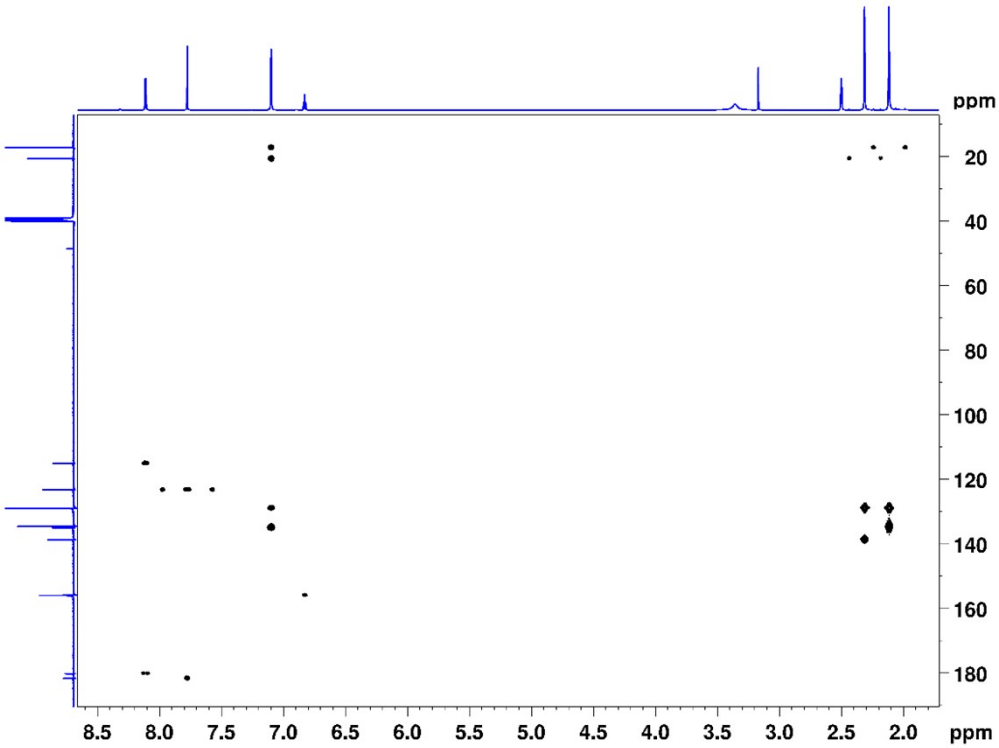

Figure S18. HMBC {^{1}H, ^{13}C} NMR Spectrum of the AuIMesSpym complex at 500 MHz (^{1}H 499.9 MHz, ^{13}C 125.7 MHz) in DMSO-d_6.

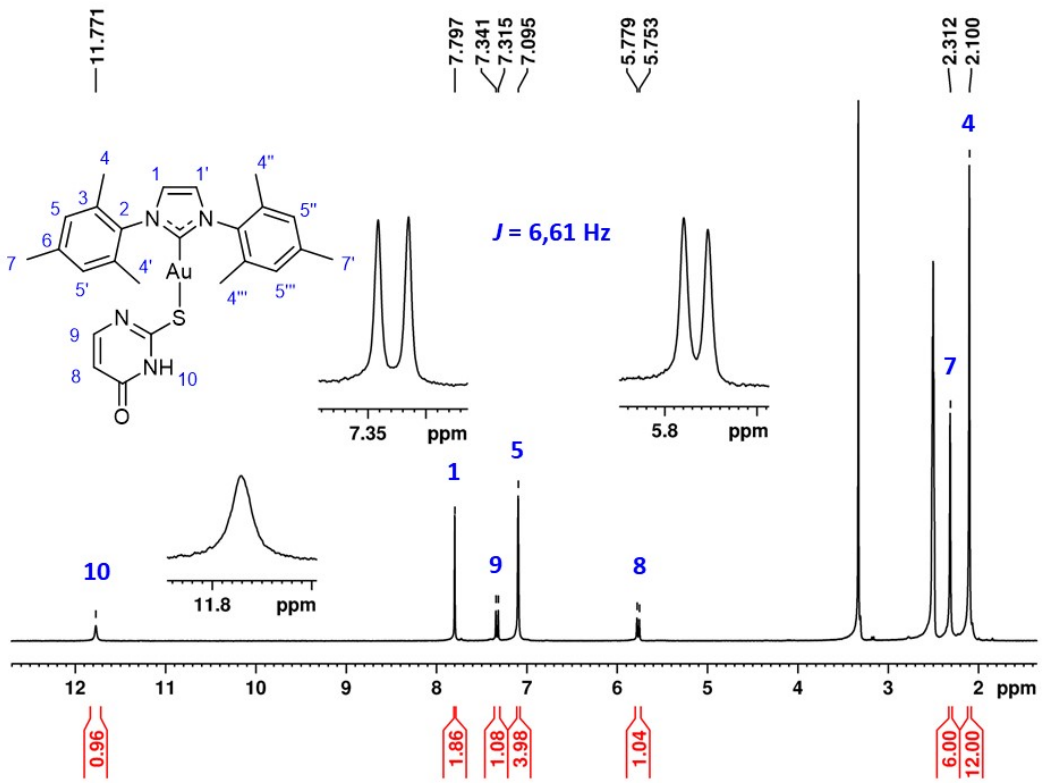

Figure S19. ^{1}H NMR spectrum of the AuIMes2tu complex in DMSO-d_6 at 250 MHz.

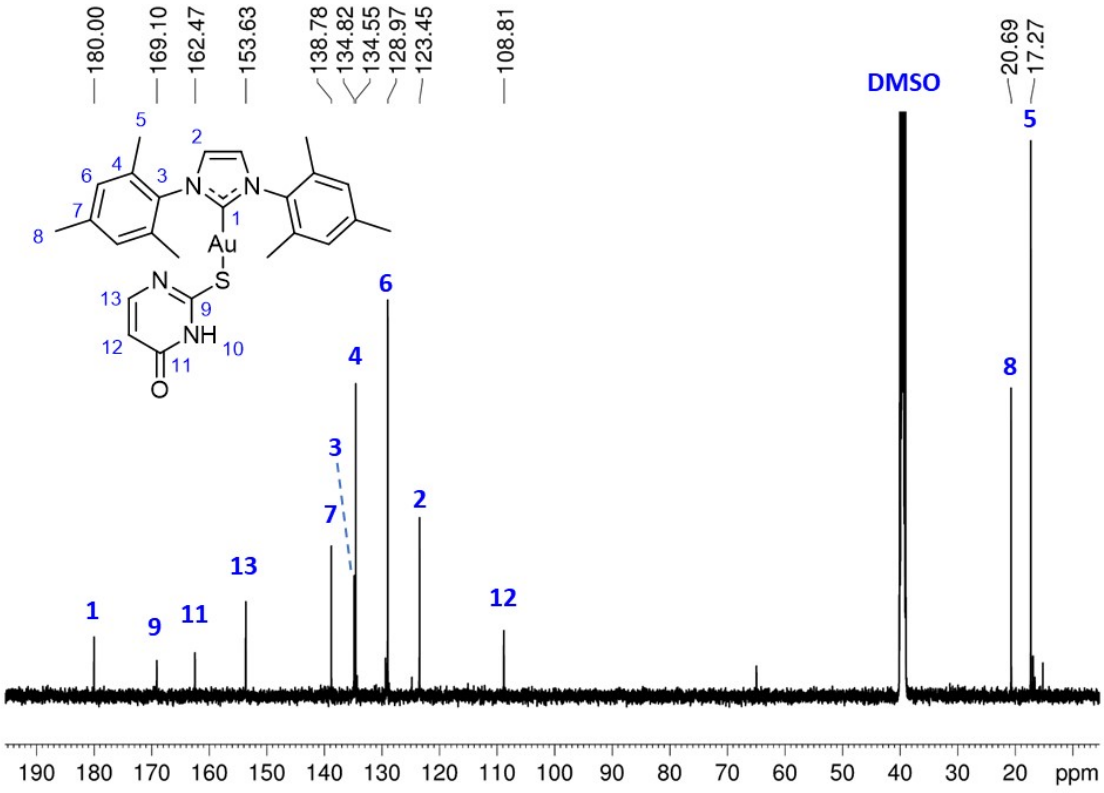

Figure S20. ^{13}C{H^{1}} NMR spectrum of the AuIMes2tu complex in DMSO-d_6 at 500 MHz (^{13}C 125.7 MHz).

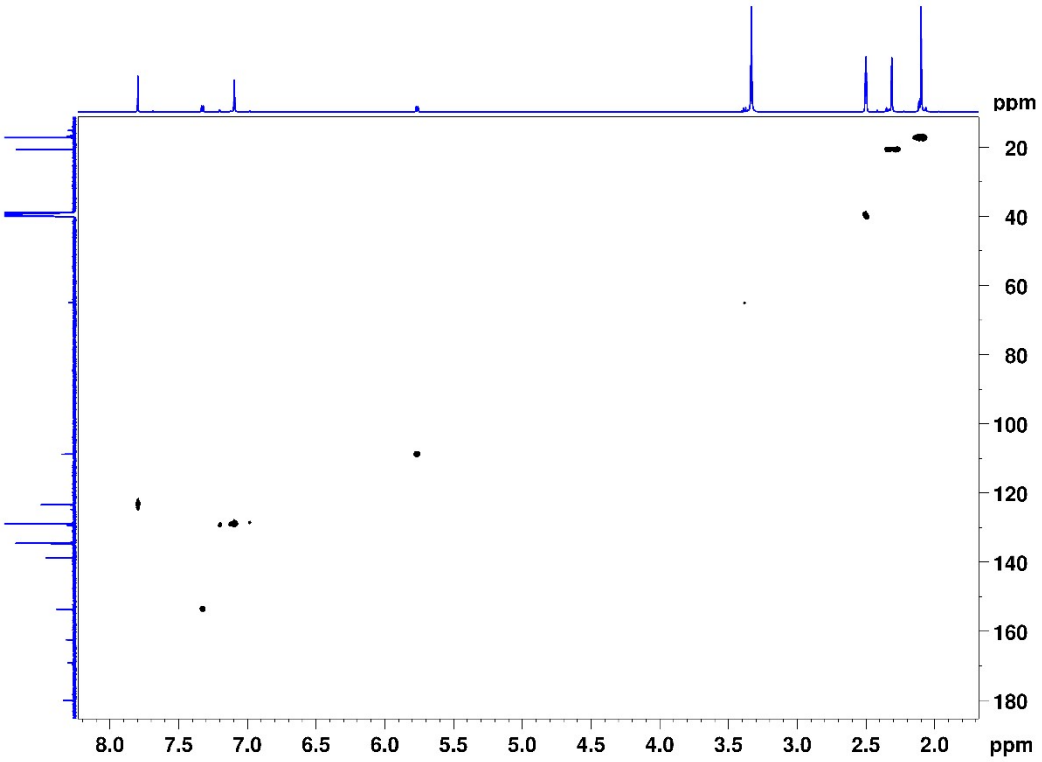

Figure S21. HSQC {^{1}H, ^{13}C} NMR Spectrum of the AuIMes2tu complex at 500 MHz in DMSO-d_6.

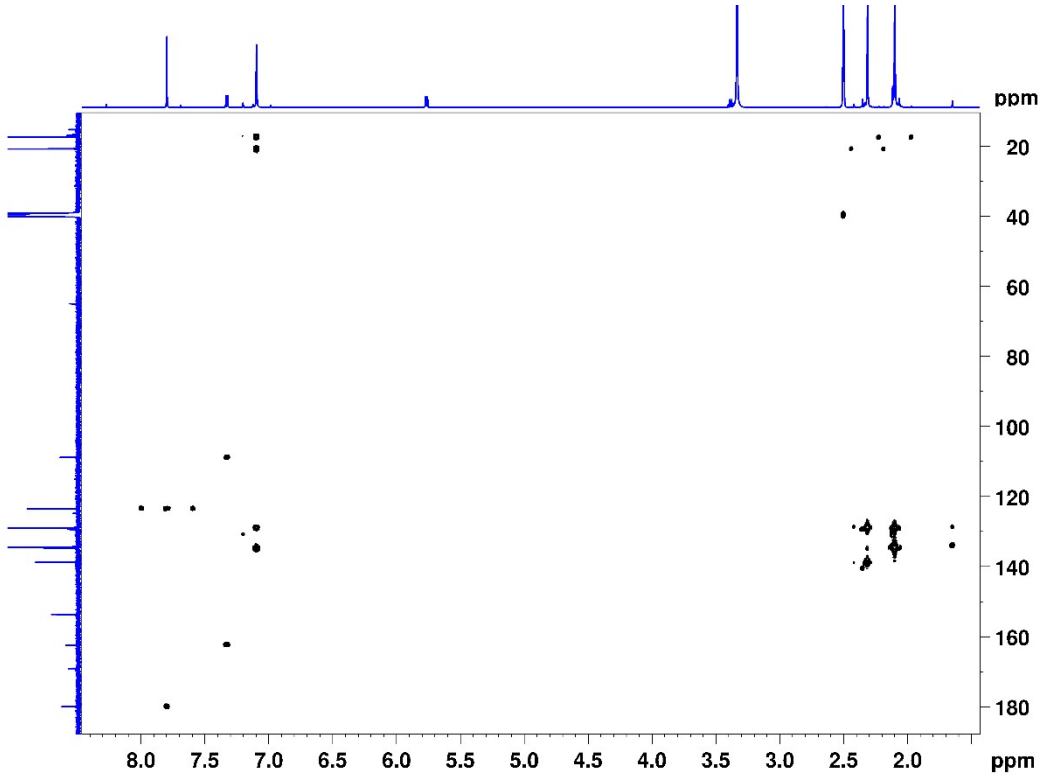

Figure S22. HMBC {^{1}H, ^{13}C} NMR Spectrum of the AuIMes2tu complex at 500 MHz in DMSO-d_6.

Complexes Characterization - HRMS

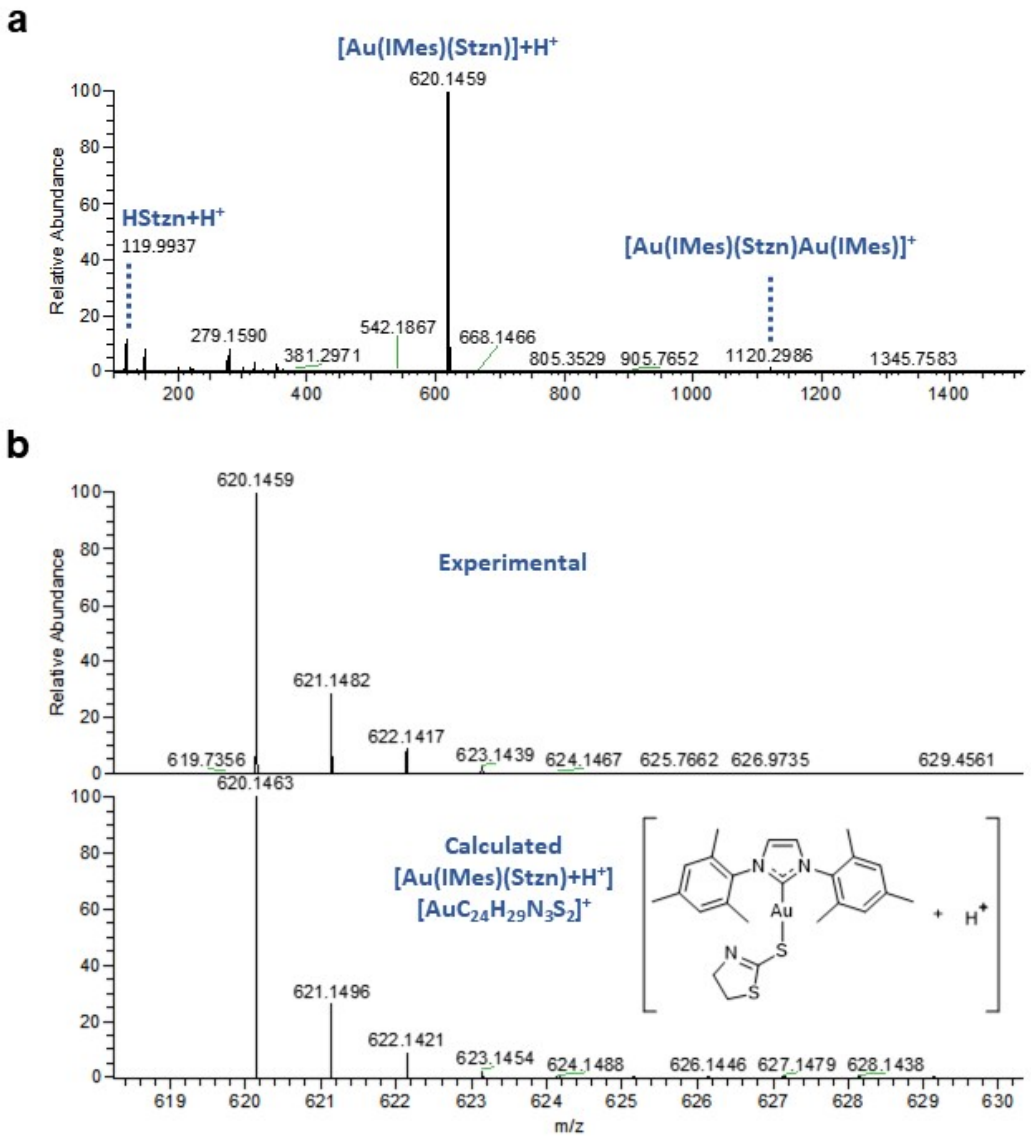

Figure S23. HRMS spectrum in ESI-MS(+) mode of the AuIMesStzn. A) Full spectrum acquired in the region 100 to 1500 m/z with respective assigned signals. B) Isotopic and calculated pattern of the molecular ion with adjusted relative intensity.

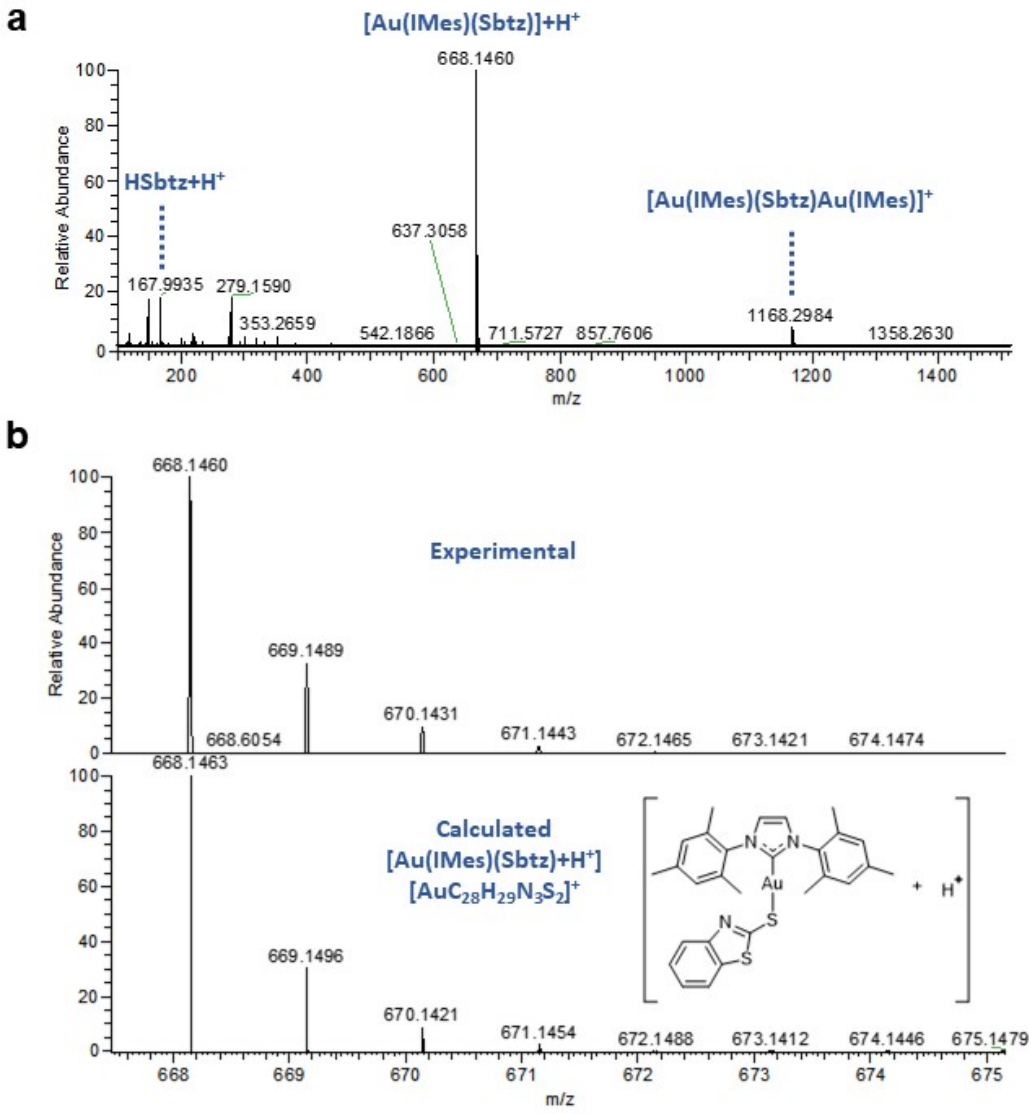

Figure S24. HRMS spectrum in ESI-MS(+) mode of the AuIMesSbtz. A) Full spectrum acquired in the region 100 to 1500 m/z with respective assigned signals. B) Isotopic and calculated pattern of the molecular ion with adjusted relative intensity.

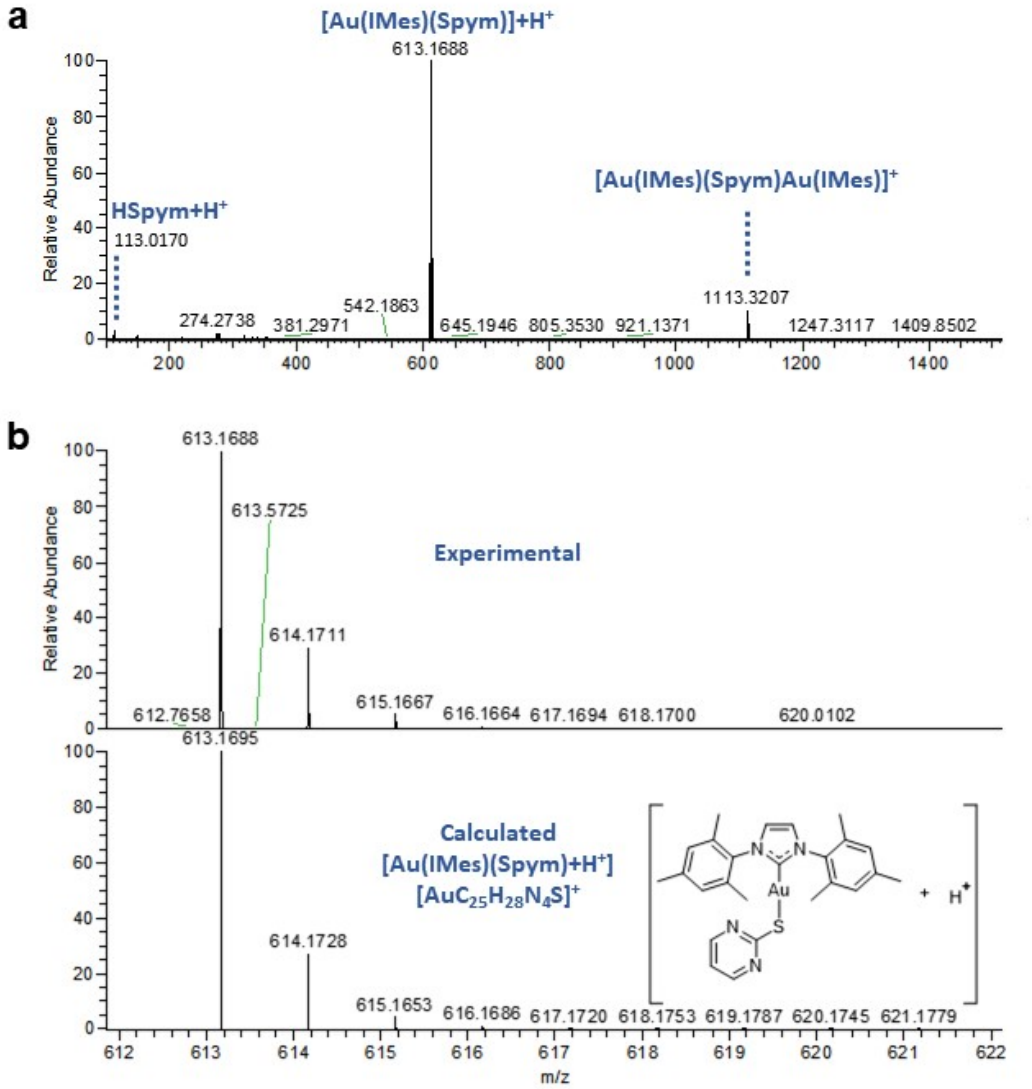

Figure S25. HRMS spectrum in ESI-MS(+) mode of the AuIMesSpym. A) Full spectrum acquired in the region 100 to 1500 m/z with respective assigned signals. B) Isotopic and calculated pattern of the molecular ion with adjusted relative intensity.

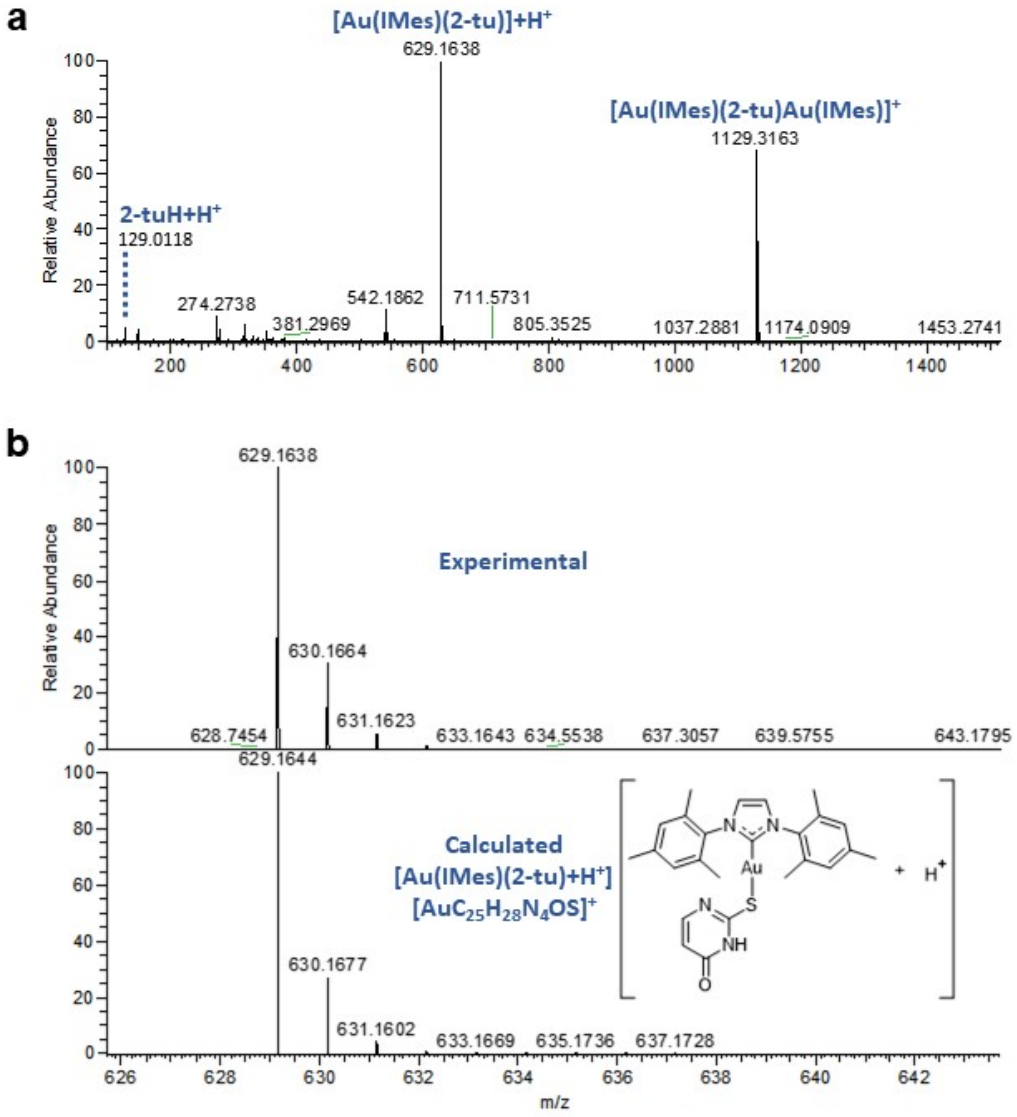

Figure S26. HRMS spectrum in ESI-MS(+) mode of the AuIMes2tu. A) Full spectrum acquired in the region 100 to 1500 m/z with respective assigned signals. B) Isotopic and calculated pattern of the molecular ion with adjusted relative intensity.

Complexes Characterization - XRD

Table S1. Crystallographic data and structure refinement for AuIMesSR complexes.

Identification code	AuIMes2tu	AuIMesSbtz	AuIMesStzn	AuIMesSpym
CCDC code	2363392	2363393	2363394	2363395
Empirical formula	$C_{25}H_{27}AuN_4OS$	$C_{29.2}H_{32.8}AuN_3O_{1.2}S_2$	$C_{24}H_{28}AuN_3S_2$	$C_{25.5}H_{29}AuN_4O_{0.5}S$
Formula weight	628.552	706.104	619.609	628.574
Temperature/K	100.15	120.00	99.99(10)	100.15
Crystal system	monoclinic	triclinic	orthorhombic	triclinic
Space group	$P2_1/c$	P-1	$P2_12_12_1$	P-1
a/Å	9.0579(1)	11.1702(12)	8.6550(2)	8.3675(1)
b/Å	21.2344(3)	15.1601(17)	14.1032(3)	16.1557(2)
c/Å	25.5964(4)	17.1723(19)	19.7630(4)	19.6651(3)
α/°	90	86.211(3)	90	99.070(1)
β/°	96.504(1)	76.397(2)	90	101.772(1)
γ/°	90	81.795(3)	90	101.630(1)
Volume/Å^3	4891.50(12)	2795.9(5)	2412.35(9)	2493.67(6)
Z	8	4	4	4
ρ_{calc}g/cm^3	1.707	1.677	1.706	1.674
μ/mm^{-1}	6.125	5.439	6.287	6.005
F(000)	2455.3	1394.6	1212.1	1231.6
Crystal size/mm^3	0.123 × 0.063 × 0.048	0.232 × 0.125 × 0.073	0.069 × 0.063 × 0.03	0.13 × 0.108 × 0.058
Radiation	Mo Kα (λ = 0.71073)	Mo Kα (λ = 0.71073)	Mo Kα (λ = 0.71073)	Mo Kα (λ = 0.71073)
2Θ range for data collection/°	4.92 to 51.36	2.44 to 54.96	5.04 to 51.34	5.06 to 51.36
Index ranges	$-13 \le h \le 12$, $-32 \le k \le 26$, $-37 \le l \le 36$	$-14 \le h \le 14$, $-19 \le k \le 19$, $-22 \le l \le 22$	$-12 \le h \le 12$, $-22 \le k \le 20$, $-30 \le l \le 29$	$-13 \le h \le 11$, $-24 \le k \le 24$, $-30 \le l \le 30$
Reflections collected	77490	44038	39732	79215
Independent reflections	9256 [R_{int} = 0.0497, R_{sigma} = 0.0522]	12827 [R_{int} = 0.0284, R_{sigma} = 0.0306]	4584 [R_{int} = 0.0445, R_{sigma} = 0.0409]	9461 [R_{int} = 0.0491, R_{sigma} = 0.0495]
Data/restraints/ parameters	9256/0/639	12827/0/625	4584/177/350	9461/0/641
Goodness-of-fit on F^2	1.030	1.004	1.054	1.023
Final R indexes [I>=2σ (I)]	R_1 = 0.0193, wR_2 = 0.0355	R_1 = 0.0207, wR_2 = 0.0393	R_1 = 0.0194, wR_2 = 0.0406	R_1 = 0.0200, wR_2 = 0.0408
Final R indexes [all data]	R_1 = 0.0252, wR_2 = 0.0365	R_1 = 0.0306, wR_2 = 0.0417	R_1 = 0.0216, wR_2 = 0.0419	R_1 = 0.0261, wR_2 = 0.0422
Largest diff. peak/hole / e Å^{-3}	0.57/-0.52	0.61/-0.61	0.67/-0.81	0.73/-0.55
Flack parameter	-	-	-0.008(5)	-

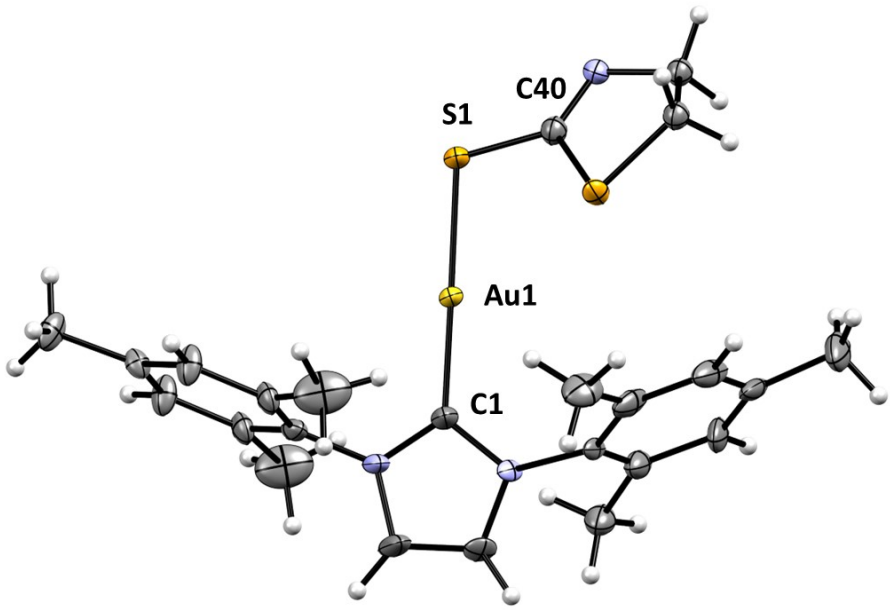

Figure S27. ORTEP diagram of the molecular structure of AuIMesStzn obtained by single crystal X-ray diffraction, ellipsoids 50% probability.

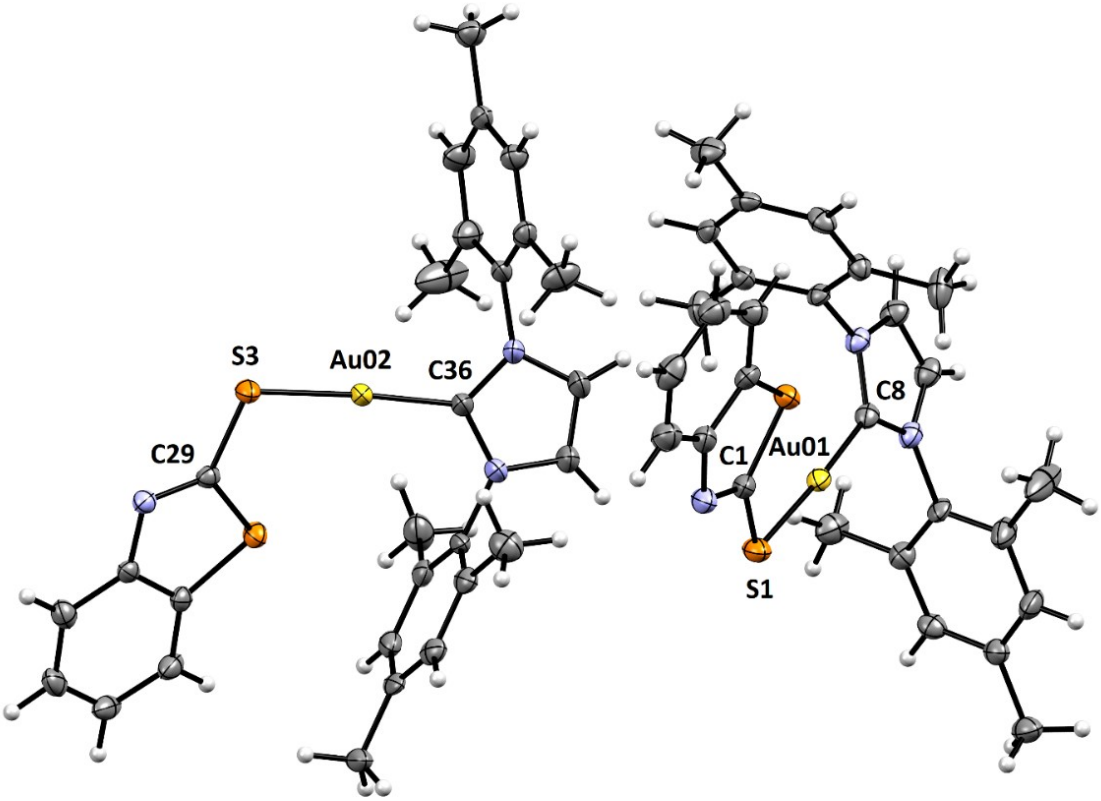

Figure S28. ORTEP diagram of the molecular structure of AuIMesSbtz obtained by single crystal X-ray diffraction, ellipsoids 50% probability.

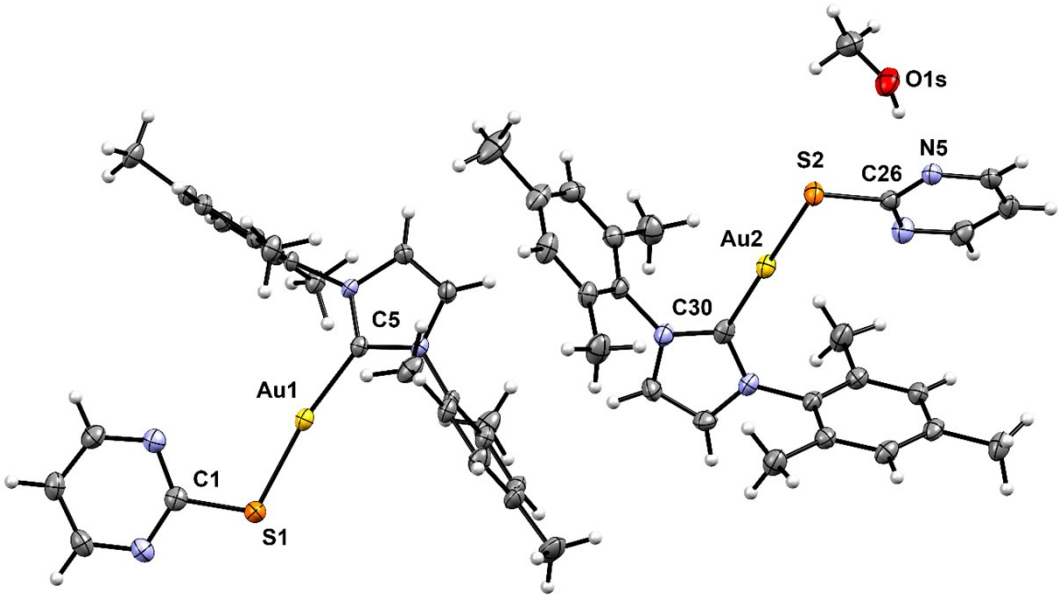

Figure S29. ORTEP diagram of the molecular structure of AuIMesSpym obtained by single crystal X-ray diffraction, ellipsoids 50% probability.

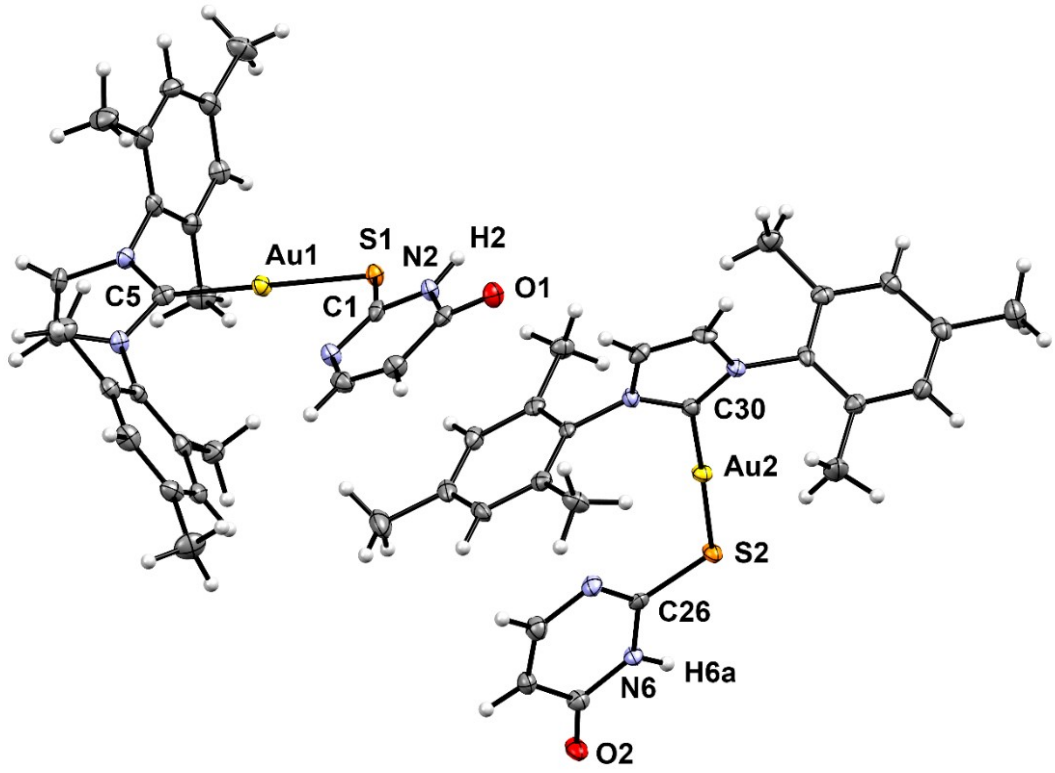

Figure S30. ORTEP diagram of the molecular structure of AuIMes2tu obtained by single crystal X-ray diffraction, ellipsoids 50% probability.

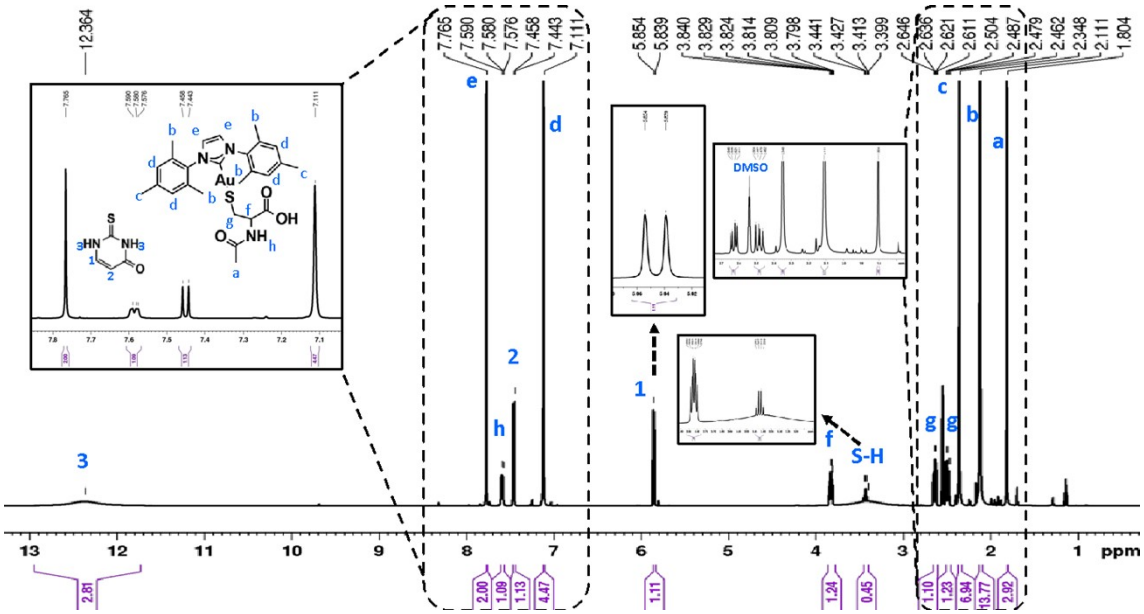

Figure S31. ^{1}H NMR of the equilibrium reaction of AuIMes2tu and NAC in DMSO-d_6. Reactants were added to the solution in 1:1 molar equivalent and let stand at 25 °C for 3 h. Spectrum was acquired in 400 MHz Bruker Avance, referenced to TMS and adjusted for solvent residual solvent DMSO at 2.58 ppm.

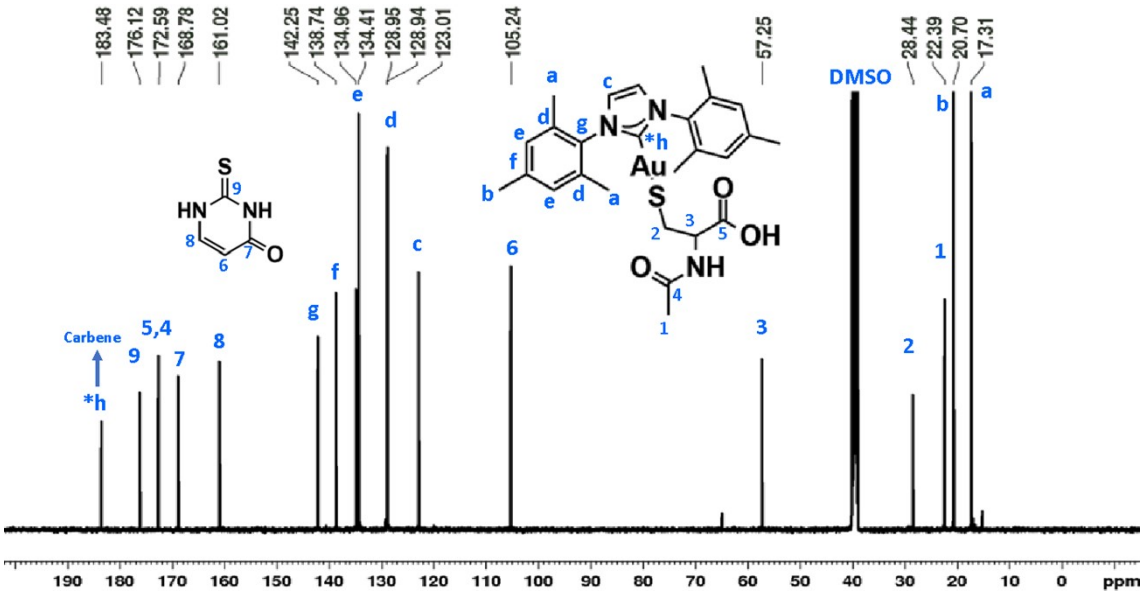

Figure S32. ^{13}C{H^{1}} NMR of the equilibrium reaction of AuIMes2-tu and NAC in DMSO-d_6. Reactants were added to the solution in 1:1 molar equivalent and let stand at 25 °C for 3 h. Spectrum was acquired in 400 MHz Bruker Avance (100.6 MHz for ^{13}C), referenced to TMS, and adjusted for solvent residual solvent DMSO at 39.52 ppm.

Steric Maps

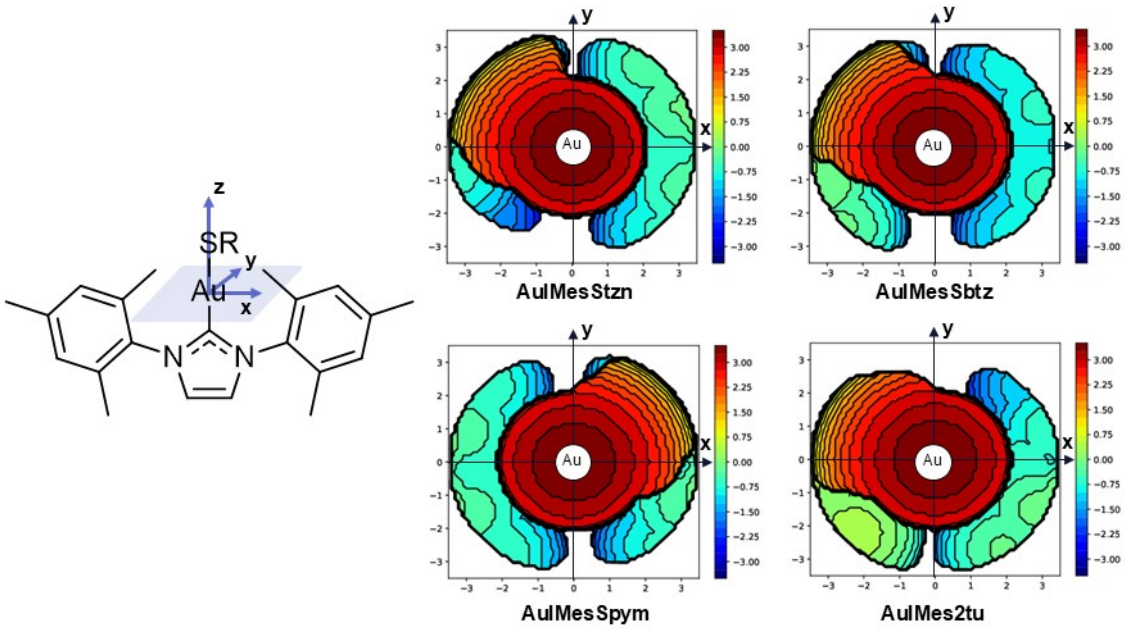

Figure S33. Schematic orientation selected for calculations using SambVca 2.1 and steric maps of IMes and SR ligands in the AuIMesSR complexes series.

Interaction Assays with Biomolecules

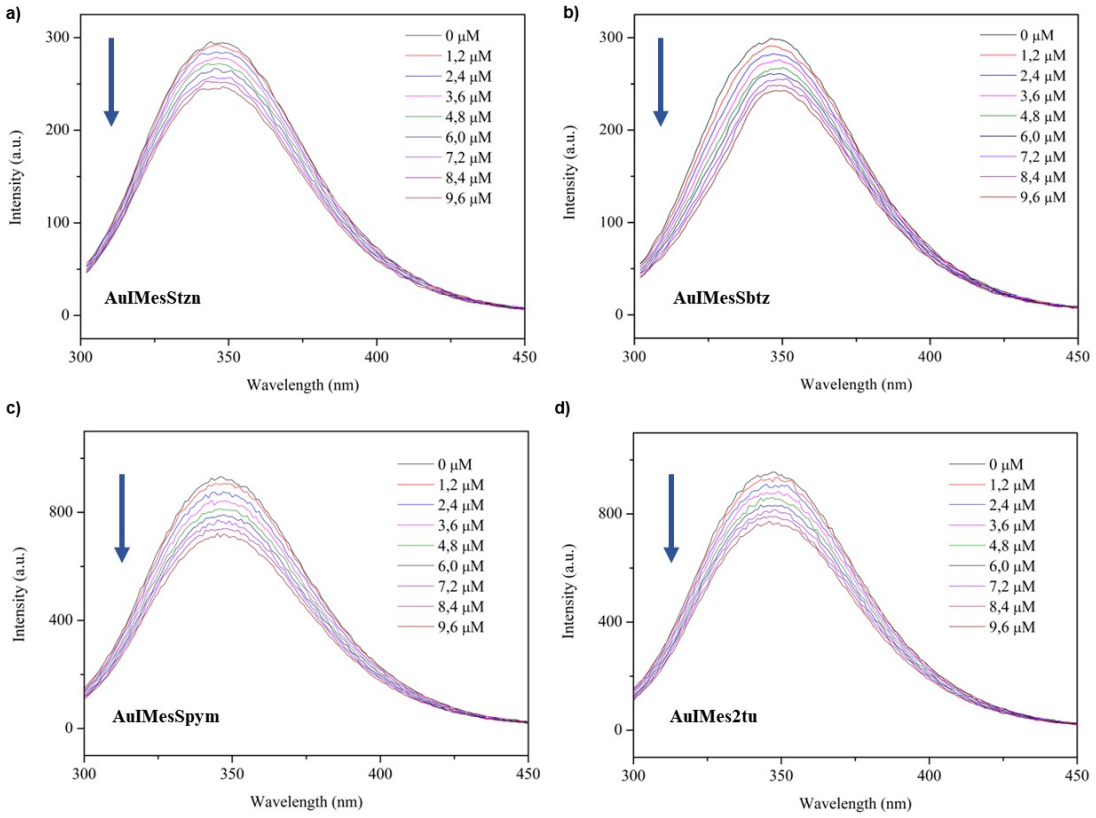

Figure S34. Fluorescence spectra showing the emission quenching of BSA solution by AuIMesSR at different concentrations. (a) AuIMesStzn, (b) AuIMesSbtz, (c) AuIMesSpym e (d) AuIMes2tu. Blue arrows indicate the decrease of emission by increasing concentrations of the quencher.

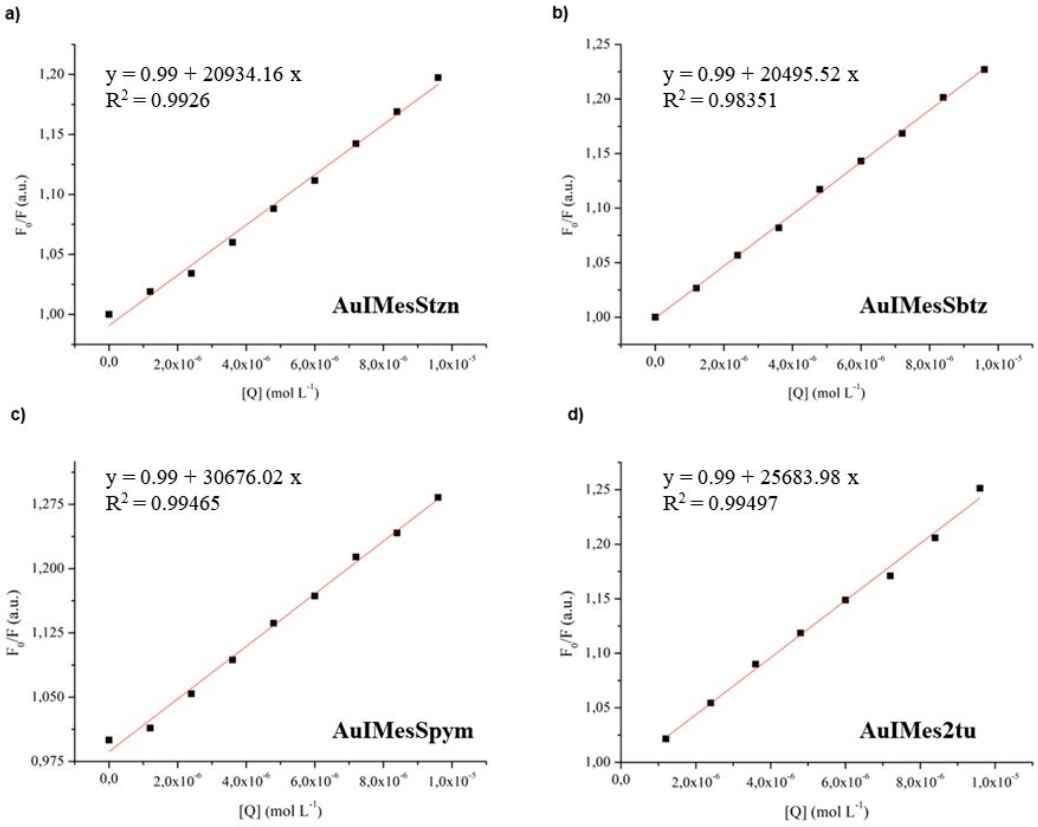

Figure S35. Stern-Volmer plot obtained for the intrinsic BSA emission at 347 nm, quenched by AuIMesSR. F_0 is the emission in the absence of quencher, F is the emission in the presence of a definite concentration of the quencher, and [Q] is the quencher's concentration. Inserts are the linear fitting data. Stern-Volmer equation is $F_0/F = 1 + K_{SV}[Q]$, where K_{SV} is the Stern-Volmer constant (a) AuIMesStzn, (b) AuIMesSbtz, (c) AuIMesSpym and (d) AuIMes2tu.

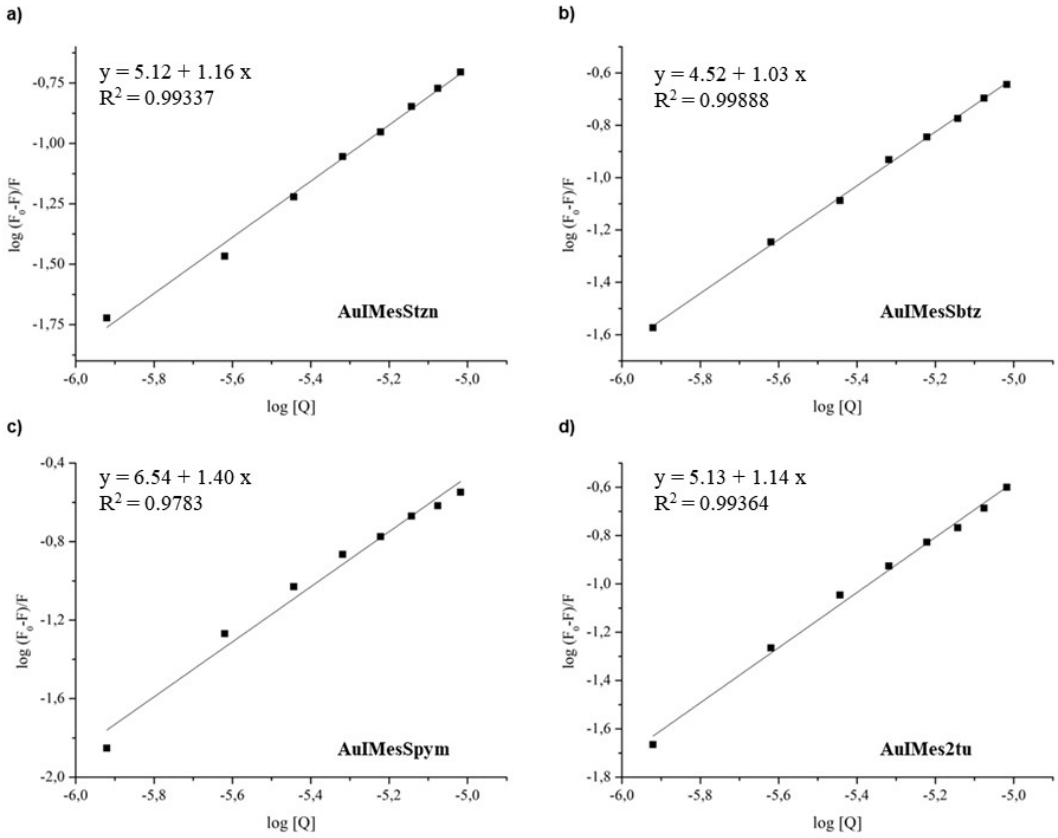

Figure S36. Scatchard plot obtained for the intrinsic BSA emission at 347 nm, quenched by AuIMesSR. F_0 is the emission in the absence of quencher, F is the emission in the presence of a definite concentration of the quencher, and [Q] is the quencher's concentration. Inserts are the linear fitting data. Scatchard equation is $log\ (F_0 - F)/F = log\ [K_b] + n\ log\ [Q]$, where K_b is the binding constant (a) AuIMesStzn, (b) AuIMesSbtz, (c) AuIMesSpym and (d) AuIMes2tu.

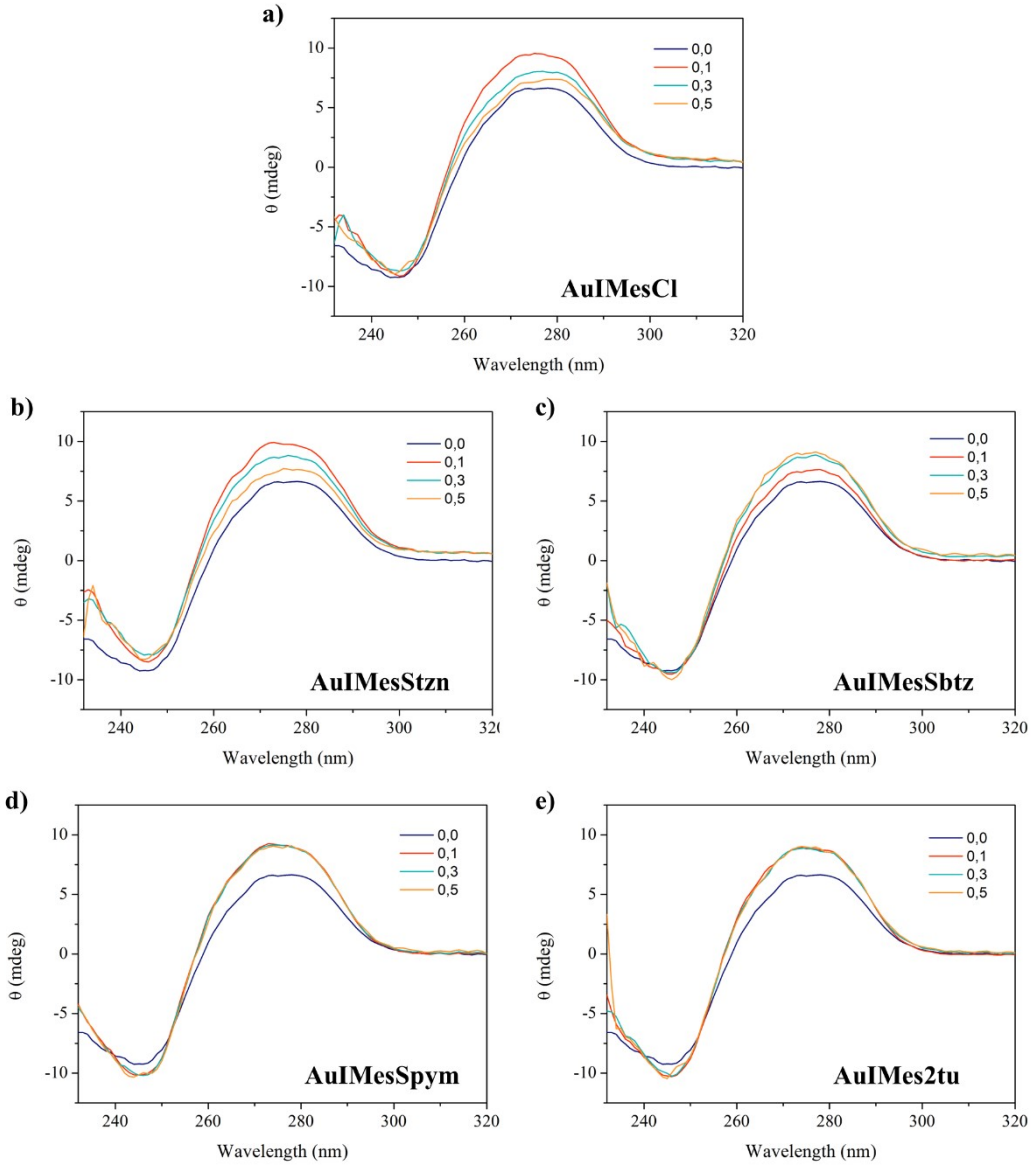

Figure S37.Circular dichroism spectra (220 nm – 320 nm) of CT-DNA (100 μM) and AuIMesSR in different concentrations (in AuIMesSR:CT-DNA molar equivalents) in phosphate buffer pH 7,4 (10 mM) (a) AuIMesCl, (b) AuIMesStzn, (c) AuIMesSbtz, (d) AuIMesSpym and (e) AuIMes2tu.

Table S2. Cell viability of Vero E6 treated with three different concentrations of AuIMesSR and AuIMesCl, accessed by MTT assay. Vero E6 cells were seeded in 96 well plates or 48 well plates, depending on the assay, incubated at 37 °C 5% CO_2 overnight when AuIMesSR and AuIMesCl were incubated for 72 h. The viability was read by MTT assay.

Compound	**Cell viability (%)**		
	50 µM	**10 µM**	**2 µM**
AuIMesSbtz	14.0	16.0	99.0
AuIMesStzn	13.9	20.2	92.0
AuIMesSpym	15.6	15.0	104.0
AuIMes2tu	12.7	29.2	96.0
AuIMesCl	25.2	86.8	94.2

DFT Optimized Structures (x, y, z coordinates)

N-Acetyl-Cysteine (NAC)

H	2.45851280440712	-2.76892614739370	9.22838367351715
S	-0.19109847820367	-0.98906713044128	10.03076375328500
N	1.74661278585639	-3.44446775093358	8.98728794347891
O	2.25670374503782	-1.44346918813253	7.25769023863559
C	1.13588079319255	-1.88081470667708	7.26687855233270
C	1.98860116647502	-4.71578792872650	9.37713797309482
O	0.17030982204650	-1.46767523563823	6.45455105086932
H	0.52060886824908	-0.76396066724734	5.88550739335008
C	0.64107619166730	-2.96721156841124	8.20538602694746
C	-0.53809389359122	-2.46883200963132	9.04938777057293
H	-0.87389720170663	-3.27126438950118	9.70571987711292
H	-1.36782846628353	-2.19516516161719	8.39720893226644
H	0.26438456839581	-3.77565466949249	7.57136646213999
H	0.70488393874427	-1.54379789176093	10.86402117192216
C	0.99808531104474	-5.77104325750858	8.97259297938049
O	2.99082776538119	-4.98528227548194	10.03068119681984
H	-0.01698725800072	-5.51323283160388	9.28053174977377
H	1.28783910623688	-6.71188411186214	9.43433781302387
H	0.99447843105109	-5.89405307793881	7.88619544147644

Au(IMes)Cl

C	2.31363211976852	-0.07749736370765	0.95436428129022
C	4.05330421503746	1.66237581769356	0.78981048579742
C	-0.40199125904310	-1.39402959961936	2.28210140271340
C	5.79379786803260	2.66119325281475	2.07640464946681
H	-1.63496703032771	-2.66397254486400	3.47338800298285
N	0.97636695711437	-0.07193199718299	0.78050797328420
N	2.70680024662923	1.18533907087126	0.69381489280578
C	4.49269855839264	2.17879744309032	2.00979927823484
C	-0.10337405728465	-0.44498033947755	3.40097488992173
C	0.53580255632504	1.18089056190640	0.41180532824707
C	1.62614533502228	1.97344038094743	0.35737405491261
H	6.15070857254586	3.06921030861128	3.01702945785533
H	-0.50434362568546	1.38917262272049	0.22590484279410
H	1.73454523530418	3.01692561234938	0.11378845591286
C	3.59767172187446	2.21675307718887	3.20972403577176
H	0.97326042646553	-0.34929336534956	3.56426947878648
H	-0.56233829819249	-0.79141621901094	4.32672688438879
H	-0.48504551880690	0.55679939569448	3.18567293192756
H	-2.61684011912588	-5.11076749173649	0.79039625947894
H	-3.31206616789859	-4.29742186560861	2.20256847054324
H	-1.87539087844308	-5.29491131302822	2.38404794242768
H	0.07381205509648	-2.59913416119638	-2.11274209956056
H	1.53181581215419	-1.90490109218544	-1.38895707987393
H	0.18077429537572	-0.85931152031044	-1.80602196235983
H	2.70089009620151	2.81332537904833	3.02125644940471
H	4.12165902811349	2.64913347161213	4.06192307657641
H	3.26176781961420	1.21349179301604	3.48537170917340
H	8.46362733430860	3.37716658127720	0.09985212666235
H	8.69325805775934	2.39675324223139	1.54844775788151
H	8.09786582483947	4.04559334929719	1.70113140902132
H	5.12943908327849	1.18317312217958	-2.41649358770725
H	3.45742665452226	1.55536214046956	-1.97080661020343
H	4.14972248280931	-0.00344339477480	-1.54299657379215

Au(IMes)2tu

H	5.87386985075859	3.10633283042737	3.81968098732626
H	-0.41201229374224	1.13492205339515	0.2913986032646
H	1.81307383571851	2.78186969374199	0.39147623286313
C	3.28317968534385	2.34722779823430	3.78429377184555
H	0.54800461458321	-0.62071018383208	4.05952344630499
H	-1.12696657213007	-0.98183590630195	4.5027863638591
H	-0.75843890100502	0.35829003959859	3.4069080747463
H	-2.81872532443251	-5.11699033200544	0.6861198733679
H	-3.22298700749020	-4.67309286062667	2.3550723637554
H	-1.81562102711305	-5.67928901751141	2.0207364522938
H	0.58006479180058	-2.79419758633669	-1.73565029069000
H	1.83018562303122	-1.92138136764093	-0.83543987187538
H	0.45001455790562	-1.04885669018154	-1.48721378972938
H	2.41028326381378	2.88493044166403	3.40584658757623
H	3.70022652153754	2.91347654317524	4.61696313600312
H	2.92663780114328	1.38694216375054	4.16792461182863
H	8.50571643087339	3.11295377767168	1.21867509280676
H	8.58792973240791	2.08388017757114	2.64640412505282
H	8.03486155286784	3.74875405717363	2.80650059485431
H	5.47015873387355	0.57685946939408	-1.42737560677608
H	3.79909745308258	1.14224520379001	-1.29610954686848
H	4.25700571324006	-0.40074868076356	-0.58890442189068
N	6.07623784167457	-1.30382167364578	4.17908613385028
C	7.19671738798923	-0.84697717689997	4.79062931197980
C	5.80082376534395	-2.57626351068930	4.33291246829722
N	6.60160360551324	-3.39055819144543	5.06897067793010
C	7.76316496923812	-2.98943119587267	5.72087726739305
C	8.04499692179953	-1.59998293378829	5.54087780781461
O	8.41836548851184	-3.80582254067246	6.36276668906947
S	4.41366317345916	-3.34455690449888	3.62523956696853
H	7.39851688829542	0.21089132695568	4.64566843679345
H	8.92619359234433	-1.17919546851129	6.00532748765172
H	6.35134245260854	-4.36691793374429	5.16321448265137

Au(IMes)Sbtz

C	4.42807651518321	1.68026305906829	3.42100227970089
H	1.53147627132826	-0.67460214375731	4.17555462420252
H	0.03375287184366	-1.06304809719231	5.03362682994481
H	0.08756018770890	0.28933916516766	3.89473198951763
H	-2.46315546487334	-5.24858639832826	1.67131077566170
H	-2.71978517529083	-4.63615671140260	3.31598462734844
H	-1.33416502517032	-5.66172439627716	2.96215733662809
H	0.09115688728274	-2.80317208665965	-1.45426829116131
H	1.60987807863458	-2.10885383577332	-0.86930356140739
H	0.21817202418284	-1.06738122632146	-1.13456836391965
H	3.47072146857794	2.20680775178938	3.43696173777514
H	5.08590439726569	2.13864918338883	4.15932036257458
H	4.23286470073905	0.64982246305912	3.73272000091858
H	8.62648546917563	2.97513761565612	-0.48607862344721
H	9.08822444464636	1.76075961294574	0.70570707916808
H	8.66826868529390	3.38504815265725	1.23917027888730
H	4.78617913243909	1.00577581953215	-2.45339835670218
H	3.29224684041332	1.61543142954449	-1.73136613837665
H	3.76823760590558	-0.05643868402954	-1.46841621534695
C	5.04143448942954	-5.29646550870863	5.73375369371100
C	4.08083503169642	-4.35851612531056	6.15997849595256
N	5.44857220397225	-5.17399043873241	4.42424057783103
S	3.70848066540479	-3.30750078838813	4.83516528726809
C	4.84543290911390	-4.18940668984129	3.83346159794129
S	5.12822334745569	-3.76248367439724	2.17883903213145
C	5.50355778630093	-6.25563449946518	6.63536955803128
C	5.00478828277007	-6.26150142568818	7.92556984007215
C	4.05125559260618	-5.32577552045530	8.33394864600130
C	3.57920655209166	-4.36446396505658	7.45459290399029
H	3.67402925747167	-5.34981286468185	9.34987801227800
H	2.83942467579619	-3.63804003674923	7.77006741581062
H	6.24338183008423	-6.98064502758515	6.31523740735183
H	5.35928215143260	-7.00400118223602	8.63159309440156

Au(IMes)Spym

C	1.75696573063858	1.71377011737474	0.58819007703547
H	5.89946939861577	3.03233167260515	3.79270740854522
H	-0.32627831801899	1.11169980832531	0.14716703880154
H	1.92982086394230	2.71650036892847	0.23514244831985
C	3.30412729645368	2.29577345684307	3.70015024922256
H	0.54135866300705	-0.43501929417407	3.99108693066691
H	-1.16193501832282	-0.66240796375939	4.41382740713077
H	-0.68826352631143	0.56535485296683	3.23052882881431
H	-2.93474322572597	-5.03516883604222	0.89861269851468
H	-3.37712506208594	-4.42609626404447	2.50492011241805
H	-2.00030383541987	-5.50922459409230	2.31491495446746
H	0.56461466326201	-3.02227519847782	-1.63407043522461
H	1.85783412318575	-2.18498230926000	-0.76233853630111
H	0.55816270124796	-1.25915027228366	-1.49973913351422
H	2.44145636320359	2.83252488540915	3.29751161438885
H	3.70461213214292	2.86851982405931	4.53652670280285
H	2.93580424010534	1.34042266293180	4.08491975574782
H	8.59121041486666	3.00689353131213	1.25451188029683
H	8.63083914000957	1.98618867420389	2.69024166336348
H	8.08607049802233	3.65583828949326	2.82624099517775
H	5.59760046346502	0.46562344998531	-1.44459645749737
H	3.94214353058514	1.08389749393715	-1.37226172315704
H	4.32742846949209	-0.46669020333928	-0.63848808353369
N	5.97793272818844	-1.42228979913595	4.32510697918501
C	7.04400367107624	-0.96869886364846	4.97548761632522
C	5.73491470429183	-2.73544362411739	4.40755121460622
N	6.48170842122519	-3.61321972579086	5.09080766800811
C	7.53935700456322	-3.13213535636798	5.73121528477408
C	7.87956917165003	-1.79013849747716	5.71106159065228
H	8.13848364405900	-3.85224183926306	6.28259837170122
S	4.35405936220590	-3.42850851656395	3.58629926208586
H	7.23300017595285	0.09928785735356	4.90148279172607
H	8.74422610364017	-1.40832726903639	6.23674857210153

Au(IMes)Stzn

C	1.83650122965493	1.65842676092917	0.76628356733757
H	6.67482648652791	2.41176560926356	3.10948999540856
H	-0.30864394796734	1.11339351725491	0.74301413964821
H	1.94996655556521	2.70238376548874	0.52704119914547
C	4.14195557629949	1.59167872533810	3.53148105467790
H	1.27173934500419	-0.83520013841325	4.03107726345986
H	-0.30311138108057	-1.16470900801507	4.76674696104602
H	-0.10111905952884	0.19767263017292	3.65630515486979
H	-2.87967352303631	-5.05909430004838	1.25654339509917
H	-2.79574256051108	-4.77293614820881	3.00515805301985
H	-1.59162620671128	-5.78699701274755	2.20977246589735
H	0.12839737128705	-2.78755933164691	-1.73806203796785
H	1.60982094145111	-2.10552337003492	-1.05109369974483
H	0.23605906507644	-1.05836950662417	-1.37958186853447
H	3.18160811452738	2.11092997609568	3.48166715155481
H	4.73461539833706	2.03927545830117	4.32919790707169
H	3.93177953278465	0.55341342558764	3.80448026535712
H	8.62627827544584	2.99160215373884	-0.01382933970340
H	9.00020418202042	1.81915359106414	1.24970258384114
H	8.49579310690660	3.44540321922440	1.69575877444143
H	4.99255900056655	0.99816880150173	-2.30023096220208
H	3.44349180057273	1.61139961680316	-1.71090990973118
H	3.88725957476638	-0.06369144944257	-1.41376641542664
C	5.07293138661267	-5.24542927245734	5.88572647324000
C	3.82784232867737	-4.42273635322247	6.23112377882015
N	5.31048842246823	-5.21875702503317	4.45225821001525
H	4.95942211691221	-6.27644543875544	6.22882814027238
H	5.95682690350804	-4.83157618393276	6.38730290526402
S	3.73529838714070	-3.18837208461564	4.90941419963141
H	3.90840731328949	-3.93001499724211	7.19923644309841
H	2.92033050990352	-5.02815793379365	6.21010582309631
C	4.75289789103739	-4.22697156450513	3.88631370725239
S	4.97639501463140	-3.83895221558564	2.20299921789156

Au(IMes)NAC

H	-2.41742348008385	-5.18730654652753	0.3837817883607
H	-2.48786801492362	-5.07783889193478	2.1525688726926
H	-1.14016560479728	-5.89743947175556	1.3709474934666
H	-0.20724421021612	-1.88980604639363	-2.1765614039555
H	1.32887172795362	-1.27213516765147	-1.55164893613858
H	-0.12730993778693	-0.29729622894110	-1.4106657479471
H	3.24874648320378	2.36893641141716	3.52348820102149
H	4.86318120382228	2.10118013848020	4.19470292680323
H	3.93003465996613	0.74775071551126	3.54155722869030
H	8.26933290616920	3.74173056402325	-0.37130812329933
H	8.79729182783129	2.54829812225610	0.81614923895476
H	8.23000452653129	4.12263618217966	1.36010223515356
H	4.47341874344333	1.95048362307676	-2.50863484853267
H	2.92961337799528	2.07655378960068	-1.65148322410925
H	3.76848899149978	0.53309076744569	-1.72046835540500
S	5.37022794549587	-3.33422077925042	0.79866140281385
O	4.54480834012157	-1.46050850409462	5.67469454719805
H	4.84192544377971	-2.18089380164971	3.38234175412845
C	5.03568732017489	-4.48268650163369	2.17684620151754
H	3.96335490663828	-4.59309262739381	2.33422007609117
N	5.08337006767559	-2.90581841733767	4.04890990982873
C	4.98948991149535	-2.55814090247844	5.34951393161781
O	7.82680731265578	-2.96373767230446	3.65327765994822
C	5.68136021016782	-4.08965699911156	3.50756155190294
H	5.43449681078857	-5.45065127595276	1.87480886886769
C	7.19276298565343	-3.94484254864452	3.36404070709357
C	5.42544028103417	-3.56853381176058	6.37297136089085
H	4.85081782909743	-4.49306976300994	6.27864077522338
H	5.26997345039881	-3.14898104635278	7.36405469779093
O	7.74144779830595	-5.06561205334569	2.89929943708382
H	5.51663369484285	-4.92511734459513	4.19570874767246
H	8.70057283880747	-4.93636898221250	2.83301858492936
H	6.48135915622850	-3.82072915198665	6.25002190090225

2tuH – thioiminol form

N	6.01999816302535	-1.38600428970848	4.18977946632673
C	7.18920988872642	-0.96675646465199	4.74648479115800
C	5.77267038625896	-2.65877219898378	4.27900128625134
N	6.60390807785276	-3.53555986646684	4.88025137200649
C	7.81661223495223	-3.17692870523651	5.47166865476416
C	8.08493645570962	-1.77397458857695	5.36983590497760
O	8.51238182555238	-4.03495586750008	5.99806484124779
S	4.31005031895415	-3.34456113000258	3.60838466405379
H	7.38064600085774	0.09868466433035	4.66406325771827
H	9.00057708695209	-1.38769684364443	5.79622965593106
H	6.36311640079503	-4.51867287927661	4.92429726396402
H	3.86315316036325	-2.16443183028208	3.15135884160075

2tuH – thioamide form

N	6.02530638634962	-1.42846948963182	4.22180862423943
C	7.17807262920815	-0.94054248199875	4.75609671491221
C	5.68020580056187	-2.73689083716661	4.26063941928559
N	6.58561848235863	-3.53568975785689	4.87249523558249
C	7.79878967934575	-3.15512544083528	5.45060054443771
C	8.07012565510867	-1.74384470157867	5.36341590334999
O	8.50976544154362	-3.99994115461374	5.96683766641437
S	4.25892907584292	-3.30843280430250	3.60794602315134
H	7.31638169090938	0.12817745347166	4.65441650711328
H	8.98411264287415	-1.35599153093180	5.78762009992086
H	6.35897765315076	-4.52105521108565	4.91826347354225
H	5.37385486274644	-0.79909404346993	3.77578978805044

SbtzH – thioiminol form

C	5.04826855403287	-5.29510924606981	5.71053918254945
C	4.08912516678418	-4.35798123562094	6.13429206542220
N	5.45388718849584	-5.16953424839102	4.39821966024276
S	3.70844903986162	-3.30200744651946	4.81644437090753
C	4.84330384407357	-4.18668858168557	3.82820170633336
S	5.06529792782605	-3.68649096482487	2.17522200259633
C	5.51253709344882	-6.25501857791641	6.60903235617559
C	5.01340119235833	-6.25883097899500	7.89802408557795
C	4.05985351691498	-5.32152099741076	8.30527766877161
C	3.58603938541878	-4.36022281485802	7.42861340527808
H	3.68356444201707	-5.34539842083335	9.32144461849981
H	2.84687895934985	-3.63355258708897	7.74379703441826
H	6.25198174541728	-6.97946145770317	6.28766004735482
H	5.36679647616975	-7.00044795821057	8.60526236009005
H	5.97771546783100	-4.63479448387203	1.90291943578217

SbtzH – thioamide form

C	5.04701467383541	-5.30667306798380	5.73825002106311
C	4.09471694763452	-4.36649837074587	6.13827447566564
N	5.41558715568799	-5.13456918360102	4.41996163549642
S	3.72008677723159	-3.30896804065253	4.80947211790392
C	4.82833752774348	-4.12987520371755	3.74820546778828
S	5.08902457237989	-3.70871209335501	2.16421380850062
C	5.51858265497212	-6.26757583078739	6.62157108913686
C	5.01430322469364	-6.26526372772408	7.91135040811251
C	4.06229095072492	-5.32851522773442	8.31301276740297
C	3.59153570169837	-4.36874952838752	7.43028012082519
H	3.68334528826252	-5.34893439943982	9.32795261815236
H	2.85204156486496	-3.63987363746684	7.73915843007677
H	6.25808353045689	-6.99339439039765	6.30434117059075
H	5.36764894026079	-7.00577015743674	8.61927813987074
H	6.09481048955291	-5.72685714056973	3.96066772941383

Spym – thioiminol form

N	5.94725633841092	-1.43905327033968	4.30723698413116
C	7.01296376310728	-0.97464617410505	4.95522801882381
C	5.73251483594233	-2.74590463500361	4.40847524098151
N	6.46570006727835	-3.62653557027307	5.08333159781257
C	7.52389964948916	-3.13738668085079	5.72157564460336
C	7.85117535390528	-1.79287596392892	5.69132072318174
H	8.12755559675088	-3.85093384461313	6.27479739880545
S	4.34795343508437	-3.44671393917962	3.58499311127929
H	7.19635378066396	0.09311208240958	4.87833553378382
H	8.71440187373006	-1.40337182371938	6.21358772925791
H	3.91211530563740	-2.29304018039632	3.05512801733935

Spym – thioamide form

N	5.98867085522480	-1.48841533235583	4.34407023395595
C	7.04405864457265	-0.95568921223188	4.97250813293594
C	5.67068996600118	-2.82305444699221	4.37947875864603
N	6.47796314081406	-3.63826486147583	5.09350231739900
C	7.51825883894159	-3.12632397265713	5.71552745706953
C	7.86454834209092	-1.76986475346385	5.69600142788271
H	8.13134552367676	-3.82897292692222	6.27425062037777
S	4.31839364934150	-3.36884474903526	3.54982963248284
H	7.18128593680695	0.11260446140888	4.86421273477344
H	8.72726540340930	-1.38618305829253	6.21965555040777
H	5.37476969912026	-0.88800114798213	3.80754313406901

Stzn – thioiminol form

C	5.08395759444544	-5.24910484973908	5.85391807341633
C	3.84485756852018	-4.42181519858719	6.19849999490991
N	5.29858316658808	-5.23896693653116	4.41273600551523
H	4.97105918617315	-6.27648608646510	6.20554342410886
H	5.97721984129670	-4.83117308872727	6.33309195589313
S	3.76471827298846	-3.17123484908007	4.88925865101321
H	3.92301427920125	-3.92947008357478	7.16660102725064
H	2.93196494543655	-5.01790280732688	6.16656968079606
C	4.73592141482891	-4.24444719593441	3.87038173014268
S	4.83606751468053	-3.80828695387907	2.18168235781533
H	5.78328621584074	-4.71263195015497	1.87880709913861

Stzn – thioamide form

C	5.10705598051754	-5.25832943539573	5.90803210538420
C	3.85825610513338	-4.44605386567749	6.20841730114851
N	5.24100452726917	-5.25123674957801	4.46314839072037
H	5.01337426236057	-6.28199187510137	6.27125955244306
H	5.99322307170129	-4.80238246901143	6.36216646143671
S	3.77898396881900	-3.22287804683213	4.86826137538906
H	3.91885218291933	-3.93624022640993	7.16785526063290
H	2.95541059528216	-5.05606738245819	6.17323002946399
C	4.73886205427567	-4.21706701141089	3.80252609200830
S	4.96942088358387	-3.85611278262132	2.19489473211696
H	5.88456636813800	-5.87380015550348	3.99575869925591

HCl

Cl	-4.61220	1.15262	0.00000
H	-3.28220	1.15262	0.0000

REFERENCES

1 H. Puschmann and O. Dolomanov, *Acta Crystallogr. Sect. A*, 2019, **75**, e766.

2 C. F. Macrae, I. Sovago, S. J. Cottrell, P. T. A. Galek, P. McCabe, E. Pidcock, M. Platings, G. P. Shields, J. S. Stevens, M. Towler and P. A. Wood, *J. Appl. Crystallogr.*, 2020, **53**, 226–235.

3 G. Sheldrick, *Acta Crystallogr. Sect. A*, 2015, **71**, 3–8.

4 I. G. R. Gutz, CurTiPot – pH and Acid–Base Titration Curves: Analysis and Simulation freeware, version 4.4.0 https://www.iq.usp.br/gutz/Curtipot_.html.

5 O. OECD, *Test No 107 Partit. Coeff. N-Octanolwater Shake Flask Method*, 1995.

6 F. Neese, *WIREs Comput. Mol. Sci.*, 2012, **2**, 73–78.

7 F. Neese, *WIREs Comput. Mol. Sci.*, 2022, **12**, e1606.

8 M. Ernzerhof and G. E. Scuseria, *J. Chem. Phys.*, 1999, **110**, 5029–5036.

9 L. M. Debefve and C. J. Pollock, *Phys. Chem. Chem. Phys.*, 2021, **23**, 24780–24788.

10 S. Kossmann and F. Neese, *J. Chem. Theory Comput.*, 2010, **6**, 2325–2338.

11 J. Tomasi, B. Mennucci and R. Cammi, *Chem. Rev.*, 2005, **105**, 2999–3094.

12 L. Falivene, R. Credendino, A. Poater, A. Petta, L. Serra, R. Oliva, V. Scarano and L. Cavallo, *Organometallics*, 2016, **35**, 2286–2293.

13 L. Falivene, Z. Cao, A. Petta, L. Serra, A. Poater, R. Oliva, V. Scarano and L. Cavallo, *Nat. Chem.*, 2019, **11**, 872–879.

14 R. L. Renberg, X. Yuan, T. K. Samuel, D. C. Miguel, I. Hamza, N. W. Andrews and A. R. Flannery, *PLoS Negl. Trop. Dis.*, 2015, **9**, e0003804.

15 P. Kumar, A. Nagarajan and P. D. Uchil, *Cold Spring Harb. Protoc.*, 2018, **2018**, pdb.prot095505.

16 S. Pathak, M. Bhardwaj, N. Agrawal and A. Bhardwaj, *Chem. Biol. Drug Des.*, 2023, **102**, 587–605.

17 N. M. Cassani, I. A. Santos, V. R. Grosche, G. M. Ferreira, M. Guevara-Vega, R. B. Rosa, L. J. Pena, N. Nicolau-Junior, A. C. O. Cintra, T. P. Mineo, R. Sabino-Silva, S. V. Sampaio and A. C. G. Jardim, *Int. J. Biol. Macromol.*, 2023, **227**, 630–640.